STATISTICS, OPTIMIZATION AND INFORMATION COMPUTING
Stat., Optim. Inf. Comput., Vol. **16**, November 2026, pp 5087–5117.
Published online in International Academic Press (www.IAPress.org)

Beyond Routine Construction: Actuarial Risk Measures, Multi-Method Estimation, and Censored Survival Modeling with the Topp–Leone–Heavy-Tailed-G Family

Wilbert Nkomo [1*], Joseph Manyemba [1], Ezekiel Chitombo [2] Takesure Nyakuamba [1], Motion Hazvinandawa [1]

[1]*Department of Applied Statistics, Manicaland State University of Applied Sciences, Mutare, Zimbabwe*
[2]*Department of Management and Entrepreneurial Sciences, Women University in Africa, Harare, Zimbabwe*

Abstract While numerous extensions of the Topp–Leone-G (TL-G) family exist, none simultaneously provide essential contributions that move beyond routine distributional construction. This study introduces the Topp–Leone–heavy-tailed-G (TL-HT-G) family to fill three specific gaps: first, exact closed-form (up to an infinite series) expressions for four major actuarial risk measures (Value at Risk, Tail Value at Risk, Tail Variance, and Tail Variance Premium); second, a systematic comparison of five estimation methods with formal ranking across sample sizes; and third, validation on both complete and censored real-world oncological datasets against multiple non-nested competing models. We derive key theoretical properties including tail asymptotics, identifiability, and analytical hazard rate shapes, and prove that the tail index is directly tunable via a single parameter—offering explicit control over tail heaviness not available in standard TL-G extensions. A large-scale Monte Carlo simulation (3,000 replications; sample sizes 25 to 800) reveals that maximum likelihood estimation consistently achieves the lowest cumulative rank across all metrics. Numerical evaluations of actuarial risk measures confirm that the TL-HT-W distribution exhibits substantially heavier tails than Kumaraswamy-Weibull, type-I heavy-tailed Weibull, and standard Weibull benchmarks. In four real-data scenarios (complete and censored leukemia and bladder cancer data), the TL-HT-W model outperforms six non-nested heavy-tailed competitors, yielding the lowest goodness-of-fit values, the highest Kolmogorov–Smirnov p-values, and excellent alignment with empirical cumulative distribution and Kaplan–Meier curves. Collectively, these features move the TL-HT-G family beyond routine construction, establishing it as a theoretically grounded, empirically superior, and ready-to-use model for high-stakes applications in actuarial science, clinical survival analysis, and reliability engineering.

Keywords Topp-Leone-heavy-Tailed-G, Tail Index, Estimation, Simulation, Actuarial Risk Measures, Censored Data, Goodness-of-fit.

AMS 2010 subject classifications 62E30; 60E05; 62E15

DOI: 10.19139/soic-2310-5070-4108

1. Introduction

Statistical distributions have been utilized in many different domains, such as engineering, reliability, health, environmental science, actuarial science, demography, and hydrology to model data for several decades. Despite the existence of numerous distributions developed by different authors in the literature, there is a need for new distributions with enhanced flexibility to cater for complex data behaviors. Furthermore, extended versions of standard distributions help accommodate data with various characteristics including multimodality, light or heavy tails. For instance, in health, duration of hospitalization (Ickowicz and Sparks [1]; Subbiah et al. [2] reliability,

*Correspondence to: Wilbert Nkomo (Email: wilbert.nkomo@staff.msuas.ac.zw). Department of Applied Statistics, Manicaland State University of Applied Sciences, Stair Guthrie Road, P. Bag 7001, Fernhill, Mutare, Zimbabwe.

ISSN 2310-5070 (online) ISSN 2311-004X (print)
Copyright © 2026 International Academic Press

and rare events Bhati and Ravi [3]) are associated with tail risks. In finance and actuarial science, accurately predicting losses that involve high fiscal values is an important issue. Modeling these events and their probability of occurrence is related to the heaviness of tails. Heavy-tailed distributions are therefore better suited for such situations (Subbiah et al. [2]; Bhati and Ravi [3]), and conventional models may not produce reliable results.

The TL-G distribution, introduced by Al-Shomrani et al. [4], is a widely recognized continuous probability distribution that serves as a foundational generator for numerous proposed distributions in the literature. Despite its utility, the TL-G distribution exhibits several limitations, such as restricted flexibility in capturing diverse datasets, inadequate modeling of extreme values, and complexities related to parameter sensitivity and interpretation. These shortcomings can lead to poor fits in certain applications and limit its effectiveness in fields like finance, survival analysis, and environmental studies. In response to these challenges, several researchers have sought to extend the TL-G distribution to enhance its applicability and address these limitations.

Recent research on TL-G extensions has demonstrated that these distributions exhibit various geometries, including both monotone and non-monotone forms in their hazard rate function (hrf). This versatility makes them valuable for modeling different types of data and scenarios in statistical applications. Notably, the findings from Topp-Leone-Harris-G family by Oluyede et al. [5], the Topp-Leone-Marshall-Olkin-Gompertz-G by Chinofunga et al. [6], the Topp-Leone Kumaraswamy Marshall-Olkin-G by Nicodéme Atchadé [7], the alpha power Topp-Leone-G distribution by Eghwerido and Ikechukwu [8], the Topp-Leone type I heavy-tailed-G power series by Nkomo et al. [9], the ToppLeone-Marshall-Olkin-Weibull by Ahmed et al. [10], the Topp-Leone odd exponential half logistic-G family developed by Chipepa and Oluyede [11], and the Type II exponentiated half-logistic Topp-Leone Marshall-Olkin-G family by Moakofi et al. [12] highlighted the diverse shapes of the hrf, emphasizing its practical implications in various fields and demonstrating flexibility. Similarly, the work on the Topp-Leone odd Burr III-G family by Moakofi et al. [13], Topp-Leone-Marshall-Olkin family by Chipepa et al. [14], extended Topp-Leone-G family by Chesneau et al. [15], weighted Topp-Leone family by Mohammad [16], Topp-Leone-Gompertz-G family by Oluyede et al. [17], Topp-Leone-Gompertz-exponentiated half logistic family by Dingalo et al. [18] and the Topp-Leone-G power series by Makubate et al. [19] further corroborated these findings, showcasing the adaptability of these distributions in statistical modeling.

Unlike the closely related TL-type-I-heavy-tailed-G power series class (by Nkomo et al. [9]), which embeds a heavy-tailed transform within the TL-G generator, integrating it with the power series and does not provide systematic multi-method comparisons, the proposed TL-HT-G family embeds the heavy-tailed-G distribution directly as the baseline of the TL-G generator. This structural difference yields several novel features absent in previous TL-extensions: (i) explicit closed-form up to an infinite series expressions for four major actuarial risk measures (Value at Risk (VaR), Tail Value at Risk (TVaR), Tail Variance (TV), and Tail Variance Premium (TVaP)); (ii) a suite of rigorously derived theoretical properties, including limiting behaviour, precise tail behaviour characterising heavy and light-tailed regimes via the parameter α, mode and shape analysis with conditions for unimodality, and analytical justification of hazard rate shapes (monotone, bathtub, unimodal) rather than reliance on numerical plots alone, (iii) a comprehensive comparison of various estimation methods with formal ranking across sample sizes; and (iv) validation on both complete and censored real-world oncological datasets.

More broadly, while numerous Topp-Leone-G (TL-G) extensions exist (for example, in the work [5] - [19]), none simultaneously provide these essential contributions for practical risk modeling and survival analysis. Thus, the motivation for this study arises from a critical and persistent gap in the literature on Topp-Leone-G (TL-G) extensions: while numerous such families exist, they typically stop at routine distributional construction and basic mathematical derivations, failing to provide the essential practical tools required for immediate adoption in high-stakes applied fields. Our review revealed that existing extensions rarely offer explicit, ready-to-use expressions for major actuarial risk measures (VaR, TVaR, TV, and TVaP), lack systematic comparisons and formal rankings of multiple estimation methods to guide practitioners on optimal parameter estimation across different sample sizes, and are inadequately validated on censored survival data—the most common data type in clinical trials and reliability studies. To address these shortcomings and move the field beyond mere construction, we develop the Topp-Leone-Heavy-Tailed-G (TL-HT-G) family, embedding the heavy-tailed-G distribution as

the baseline of the TL-G generator to provide explicit control over tail heaviness via a single parameter, and deliver a comprehensive framework that integrates rigorous theoretical properties, closed-form actuarial measures, a definitive guide to estimation method selection through large-scale simulation, and robust empirical validation on both complete and censored oncological datasets, thereby establishing a truly application-ready model for actuarial science, clinical survival analysis, and reliability engineering.

The paper is organized as follows: Section 2 presents the development of the new FoDs, encompassing sub-families and specific instances tailored to baseline or parent distributions. Section 3 examines the theoretical properties of the the TL-HT-G FoDs while Section 4 highlights its key statistical properties. Parameter estimation is addressed in Section 5, and Section 6 delves into the examination of risk measures. Section 7 presents the outcomes of simulations, whereas Section 8 provides illustrative examples utilizing real-world data. Section 9 serves as the concluding section, providing a comprehensive summary of the research findings and an extensive discussion on the implications and potential impact of the study.

2. The New Family of Distributions

In their work, Al-Shomrani et al. [4] introduced the TL-G FoDs, characterized by the cumulative distribution function (cdf) given by

$$F(y;b,\varsigma) = \left[1-\bar{G}^2(y;\varsigma)\right]^b, \tag{1}$$

and the corresponding probability density function (pdf) is given by

$$f(y;b,\varsigma) = 2bg(y;\varsigma)\bar{G}(y;\varsigma)\left[1-\bar{G}^2(y;\varsigma)\right]^{b-1}, \tag{2}$$

where $b>0$ is a shape parameter, $y>0$ and ς is the parameter vector derived from the baseline distribution $G(.)$, and $\bar{G}(y;\varsigma)=1-G(y;\varsigma)$. The TL-G distribution is a flexible probability distribution characterized by varying skewness, specific support intervals, calculable moments, and applicability in reliability engineering, finance, quality control, and health sciences.

Zhao et al. [20] proposed the heavy-tailed-G (HT-G) FoDs defined by their cdf and pdf as presented in Equations (3) and (4), respectively as follows:

$$F(y;\alpha,\vartheta) = 1-\left(\frac{\bar{G}(y;\vartheta)}{1-(1-\alpha)G(y;\vartheta)}\right)^{\alpha}, \tag{3}$$

and

$$f(y;\alpha,\vartheta) = \frac{\alpha^2 g(y;\vartheta)\left[\bar{G}(y;\vartheta)\right]^{\alpha-1}}{\left[1-(1-\alpha)G(y;\vartheta)\right]^{\alpha+1}}, \tag{4}$$

where $\alpha>0$ doubles as a shape and tilt parameter,$y>0$ and ϑ is the parameter vector stemming from the baseline distribution $G(.)$. We shall set $D_G(y;\alpha,\vartheta)=1-\left(\frac{\bar{G}(y;\vartheta)}{1-(1-\alpha)G(y;\vartheta)}\right)^{2\alpha}$ in this article.

The TL-HT-G FoDs is derived by substituting the baseline cdf in Equation (1) with the HT-G distribution. The resulting TL-HT-G FoDs is characterized by the following statistical functions: the cdf, survival function (sf), and pdf respectively defined by

$$F(y;b,\alpha,\vartheta) = \left[D_G(y;\alpha,\vartheta)\right]^b, \tag{5}$$

$$S(y;b,\alpha,\vartheta) = 1-\left[D_G(y;\alpha,\vartheta)\right]^b, \tag{6}$$

and

$$f(y;b,\alpha,\vartheta) = 2b\alpha^2 \left[D_G(y;\alpha,\vartheta)\right]^{b-1} \frac{g(y;\vartheta)\left[\bar{G}(y;\vartheta)\right]^{2\alpha-1}}{\left[1-(1-\alpha)G(y;\vartheta)\right]^{2\alpha+1}}, \tag{7}$$

where $b,\alpha,y>0$, and ϑ is the parameter vector coming from the baseline distribution. The hrf of the TL-HT-G FoDs, defined in Equation (8), quantifies the instantaneous failure risk for a system or subject conditional on survival up to time y. It is formulated as:

$$h(y;b,\alpha,\vartheta) = \frac{2b\alpha^2 \left[D_G(y;\alpha,\vartheta)\right]^{b-1}}{\left(1-\left[D_G(y;\alpha,\vartheta)\right]^{b}\right)} \frac{g(y;\vartheta)\left\{\bar{G}(y;\vartheta)\right\}^{2\alpha-1}}{\left[1-(1-\alpha)G(y;\vartheta)\right]^{2\alpha+1}}. \tag{8}$$

2.1. Special Cases

By specifying $G(y;\vartheta)$ and $g(y;\vartheta)$ in Equations (5) and (7), this subsection illustrates various unique TL-HT-G FoDs' special cases. We take the baseline or parent cdf to be Weibull, Burr XII, and Kumaraswammy distributions.

2.1.1. Topp-Leone-Heavy-Tailed-Weibull Distribution Given the Weibull distribution with cdf $G(y;\lambda,\omega)=1-\exp(-\lambda y^{\omega})$ and pdf $g(y;\lambda,\omega)=\lambda\omega y^{\omega-1}\exp(-\lambda y^{\omega})$, for $\lambda,\omega,y>0$, as the parent distribution, and introducing $D_A(y;\alpha,\lambda,\omega)=1-\left(\frac{\exp(-\lambda y^{\omega})}{1-(1-\alpha)(1-\exp(-\lambda y^{\omega}))}\right)^{2\alpha}$, we obtain the Topp-Leone-Heavy-Tailed-Weibull (TL-HT-W) distribution with cdf

$$F(y;b,\alpha,\lambda,\omega)=\left[D_A(y;\alpha,\lambda,\omega)\right]^{b},$$

and pdf

$$f(y;b,\alpha,\lambda,\omega) = 2b\alpha^2\lambda\omega y^{\omega-1}\exp(-\lambda y^{\omega})\frac{\left[D_A(y;\alpha,\lambda,\omega)\right]^{b-1}\left(\exp(-\lambda y^{\omega})\right)^{2\alpha-1}}{\left[1-(1-\alpha)(1-\exp(-\lambda y^{\omega}))\right]^{2\alpha+1}}$$

for $b,\alpha,\lambda,\omega,y>0$. The TL-HT-W's hrf is

$$h(y;b,\alpha,\lambda,\omega) = \frac{2b\alpha^2\lambda\omega y^{\omega-1}\exp(-\lambda y^{\omega})}{1-\left[D_A(y;\alpha,\lambda,\omega)\right]^{b}}\left(\frac{\left[D_A(y;\alpha,\lambda,\omega)\right]^{b-1}\left(\exp(-\lambda y^{\omega})\right)^{2\alpha-1}}{\left[1-(1-\alpha)(1-\exp(-\lambda y^{\omega}))\right]^{2\alpha+1}}\right).$$

Figure 1 (a) displays various shapes observed in the TL-HT-W density, including reversed-J, almost symmetric, right-skewed, and left-skewed shapes. The hrf of the TL-HT-W distribution illustrated in Figure 1 (b) exhibit different geometries, which can be either monotonic or non-monotonic.

2.1.2. Topp-Leone-Heavy-Tailed-Burr XII Distribution Considering the Burr XII distribution with the cdf $G(y;c,k)=1-(1+y^{c})^{-k}$ and pdf $g(y;c,k)=\frac{cky^{c-1}}{(1+y^{c})^{k+1}}$ as the baseline distribution, where $y,c,k>0$ and introducing an adjustment term $D_B(y;\alpha,c,k)=1-\left(\frac{(1+y^{c})^{-k}}{1-(1-\alpha)(1-(1+y^{c})^{-k})}\right)^{2\alpha}$, we obtain the Topp-Leone-Heavy-Tailed-Burr XII (TL-HT-Burr XII) distribution with cdf given by

$$F(y;b,\alpha,c,k)=\left[W_B(y;\alpha,c,k)\right]^{b}$$

and pdf

$$f(y;b,\alpha,c,k) = 2bck\alpha^2\frac{\left[D_B(y;\alpha,c,k)\right]^{b-1}y^{c-1}(1+y^{c})^{1-2\alpha k}}{\left[1-(1-\alpha)(1-(1+y^{c})^{-k})\right]^{2\alpha+1}},$$

for $b,\alpha,c,k,y>0$. The hrf is

$$h(y;b,\alpha,c,k) = \frac{2bck\alpha^2\left[D_B(y;\alpha,c,k)\right]^{b-1}}{1-\left[D_B(y;\alpha,c,k)\right]^{b}}\left(\frac{y^{c-1}(1+y^{c})^{1-2\alpha k}}{\left[1-(1-\alpha)(1-(1+y^{c})^{-k})\right]^{2\alpha+1}}\right).$$

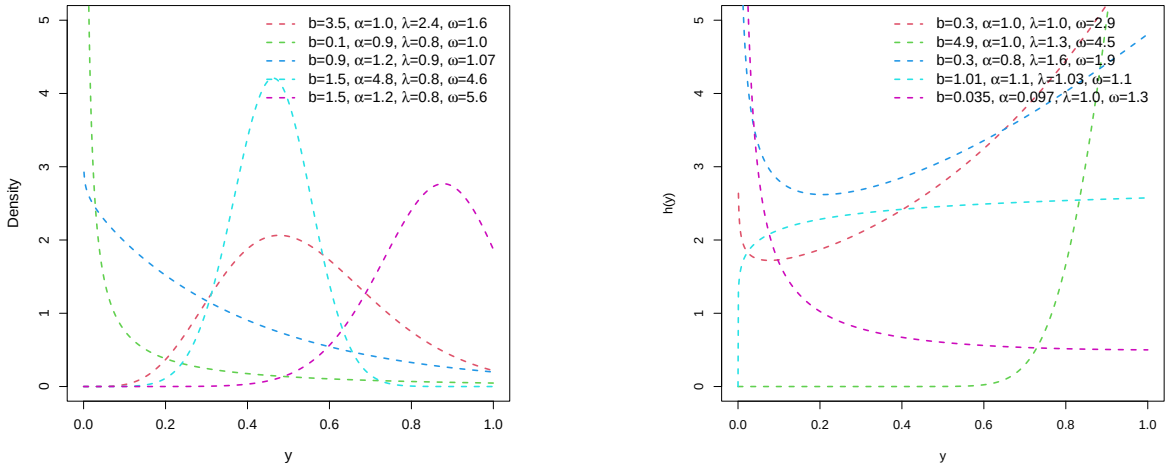

Figure 1. Some Plots of the TL-HT-W distribution's density (a) and hrf (b)

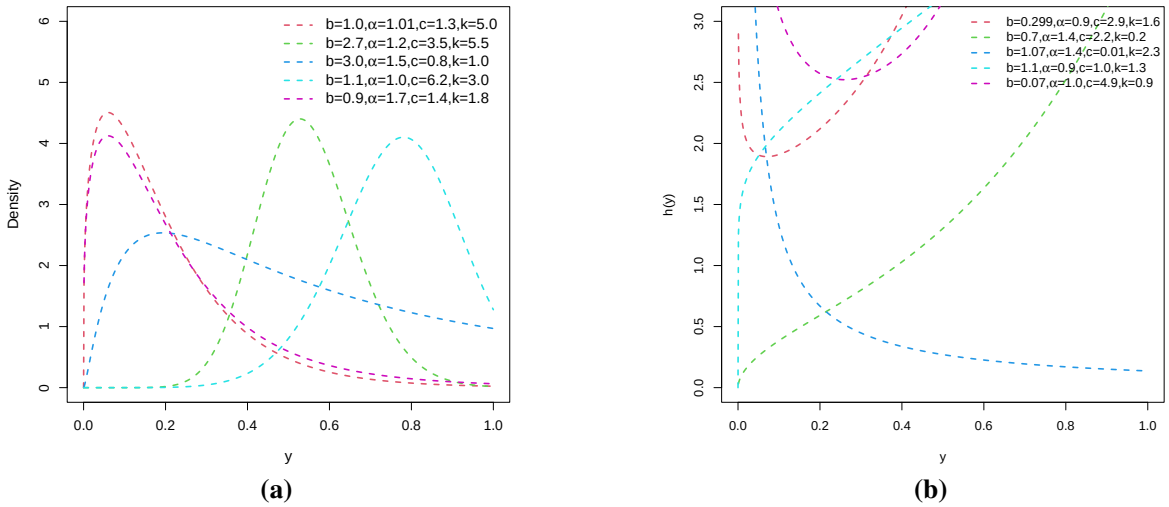

Figure 2. Plots depicting the density (a) and hrf (b) of the TL-HT-Burr XII distribution

The Topp-Leone-Heavy-Tailed-log-logistic (TL-HT-LLoG) distribution is derived when the parameter k is set to 1, while the Topp-Leone-Heavy-Tailed-Lomax (TL-HT-Lom) distribution is obtained when the parameter c is set to 1.

Figures 2 (a) and (b) respectively present the density and hrf plots for the TL-HT-Burr XII distribution. The density plot showcases different data shapes, including positively skewed, negatively skewed, and virtually symmetric shapes. The hrf plot demonstrates the distribution's versatility in accommodating decreasing, increasing, and bathtub-shaped geometries.

2.1.3. Topp-Leone-Heavy-Tailed-Kumaraswamy Distribution If we examine the Kumaraswamy distribution with cdf $G(y;a,s) = 1-(1-y^a)^s$ and pdf $g(y;a,s) = asy^{a-1}(1-y^a)^{s-1}$, respectively for $a, s > 0$, $0 < y < 1$, and

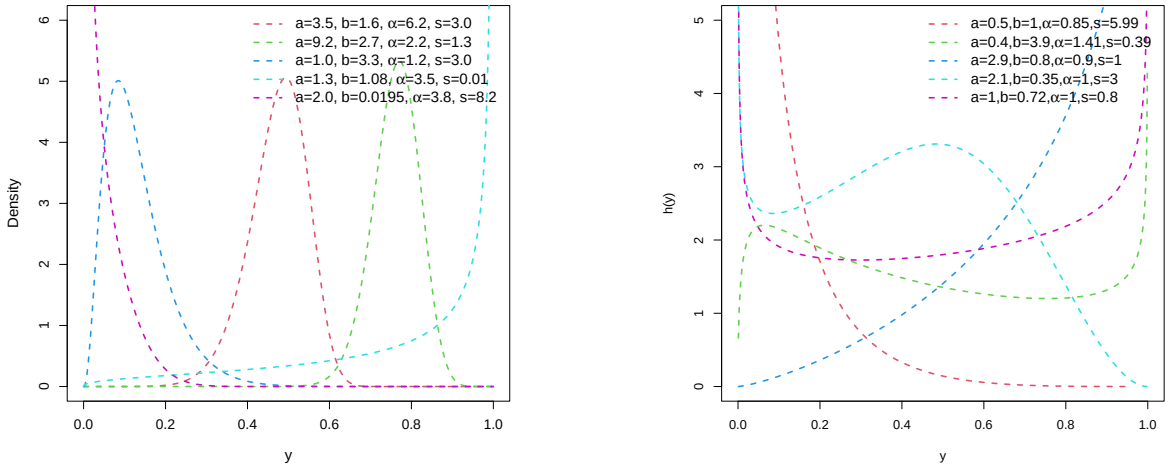

Figure 3. Plots illustrating the density (a) and hrf (b) of the TL-HT-Kum distribution

letting $D_D(y;a,\alpha,s) = 1 - \left(\frac{(1-y^a)^s}{1-(1-\alpha)(1-(1-y^a)^s)}\right)^{2\alpha}$, we obtain the Topp-Leone-Heavy-Tailed-Kumaraswamy (TL-HT-Kum) distribution with cdf

$$F(y;a,b,\alpha,s) = [D_D(y;a,\alpha,s)]^b$$

and pdf

$$f(y;a,b,\alpha,s) = 2abs\alpha^2 y^{a-1}(1-y^a)^{s-1}\frac{[D_D(y;a,\alpha,s)]^{b-1}(1-y^a)^{s(2\alpha-1)}}{[1-(1-\alpha)(1-(1-y^a)^s)]^{2\alpha+1}},$$

respectively, for $a,b,\alpha,s>0$ and $0<y<1$. The hrf is

$$h(y;a,b,\alpha,s) = \frac{2abs\alpha^2 y^{a-1}(1-y^a)^{s-1}}{1-[D_D(y;a,\alpha,s)]^b}\left(\frac{[D_D(y;a,\alpha,s)]^{b-1}(1-y^a)^{s(2\alpha-1)}}{[1-(1-\alpha)(1-(1-y^a)^s)]^{2\alpha+1}}\right).$$

Figure 3 (a) shows the density, while panel (b) depicts the corresponding hrf of the TL-HT-Kum distribution. The density plot reveals diverse data shapes, such as left and right-skewed, J and reversed-J as well as almost symmetric shapes. The hrf exhibits distinct patterns, including monotonic as well as nonmonotonic highlighting the distribution's versatility.

3. Theoretical Properties

This section provides analytical results complementing the numerical plots, including limiting behaviour of the density and hazard functions, tail heaviness characterization, parameter identifiability, and conditions for modality and hazard shapes.

3.1. Limiting Behaviour

Let $f(y;b,\alpha,\theta)$ and $h(y;b,\alpha,\theta)$ be the pdf and hrf defined in Equations (7) and (8), respectively. For any baseline cdf $G(y;\theta)$ satisfying $G(0^+)=0$ and $G(y)\to 1$ as $y\to\infty$, the following limits hold.

As $y \to 0^+$:
Assuming $g(y;\theta) \sim c_0 y^k$ and $G(y;\theta) \sim c_1 y^{k+1}$ as $y \to 0^+$ (Weibull-like behaviour), we obtain:

$$f(y) \sim 2b\alpha^2 c_0 y^k \cdot 1 \cdot [1]^{b-1} \cdot 1 = 2b\alpha^2 c_0 y^k,$$

and

$$h(y) \sim 2b\alpha^2 c_0 y^k.$$

Thus, near zero, the TL-HT-G family inherits the baseline's behaviour, with the shape parameter k determining whether $f(0) = 0$ (if $k > 0$), $f(0) = 2b\alpha^2 c_0$ (if $k = 0$), or $f(0) \to \infty$ (if $k < 0$).
As $y \to \infty$:
Since $G(y) \to 1$ and $\bar{G}(y) \to 0$, we have $D_G(y;\alpha,\theta) \to 1$. Consequently,

$$f(y) \sim 2b\alpha^2 \frac{g(y;\theta)[\bar{G}(y;\theta)]^{2\alpha-1}}{[1-(1-\alpha)]^{2\alpha+1}} = 2b\alpha^2 \frac{g(y;\theta)[\bar{G}(y;\theta)]^{2\alpha-1}}{\alpha^{2\alpha+1}}.$$

If $\bar{G}(y) \sim cy^{-\gamma}$ (Pareto-type tail) or $\bar{G}(y) \sim e^{-\lambda y^\omega}$ (Weibull-type tail), the tail behaviour of $f(y)$ is dominated by $[\bar{G}(y)]^{2\alpha-1}$. For $\alpha > 0.5$, the tail decays faster than the baseline; for $\alpha < 0.5$, the tail decays more slowly (heavier); for $\alpha = 0.5$, the tail decay rate equals the baseline.

3.2. Tail Asymptotics and Heavy-Tail Characterization

Proposition 1 (Tail Heaviness)
Let $\bar{F}(y) = 1 - [D_G(y;\alpha,\theta)]^b$ be the survival function of the TL-HT-G family. As $y \to \infty$,

$$\bar{F}(y) \sim b\left(\frac{\bar{G}(y)}{\alpha}\right)^{2\alpha} \quad \text{provided } \bar{G}(y) \to 0.$$

Proof
Using $1 - u^b \sim b(1-u)$ as $u \to 1^-$, and

$$D_G(y) = 1 - \left(\frac{\bar{G}(y)}{1-(1-\alpha)G(y)}\right)^{2\alpha} \sim 1 - \left(\frac{\bar{G}(y)}{\alpha}\right)^{2\alpha},$$

we obtain the result. □

Corollary 1
If the baseline G has a regularly varying tail (i.e., $\bar{G}(y) \sim y^{-\xi}L(y)$ with $\xi > 0$ and $L(y)$ slowly varying), then

$$\bar{F}(y) \sim b\alpha^{-2\alpha} y^{-2\alpha\xi}[L(y)]^{2\alpha}.$$

Hence, the TL-HT-G family preserves regular variation, and the tail index becomes $2\alpha\xi$. For $\alpha > 0.5$, the tail is lighter than the baseline; for $\alpha < 0.5$, it is heavier. This demonstrates that α directly controls tail weight, providing explicit heavy-tail tunability.

Corollary 2
If the baseline is light-tailed (e.g., Weibull with shape $\omega > 1$ or exponential), then $\bar{F}(y)$ remains light-tailed but with modified rate: for Weibull baseline $\bar{G}(y) = e^{-\lambda y^\omega}$, we have

$$\bar{F}(y) \sim b\alpha^{-2\alpha} e^{-2\alpha\lambda y^\omega},$$

i.e., a Weibull tail with the same shape ω but scale multiplied by 2α. Thus, the family can generate lighter or heavier Weibull tails depending on α.

3.3. Identifiability of Parameters

A model is identifiable if distinct parameter values yield distinct distributions.

Proposition 2 (Identifiability)
Let $F_1(y) = [D_G(y;\alpha_1,\theta_1)]^{b_1}$ and $F_2(y) = [D_G(y;\alpha_2,\theta_2)]^{b_2}$ be two TL-HT-G cdfs with the same baseline family $G(y;\theta)$ (where θ is a vector). If $F_1(y) = F_2(y)$ for all y in an interval, then $b_1 = b_2$, $\alpha_1 = \alpha_2$, and $\theta_1 = \theta_2$, provided the baseline family is identifiable.

Proof
Taking $y \to \infty$, we have $F(y) \to 1$, which does not discriminate. Consider y such that $G(y) = u \in (0,1)$. The equation

$$\left[1 - \left(1 - \frac{1-u}{1-(1-\alpha)u}\right)^{2\alpha}\right]^{b} = \text{constant}$$

for all u forces $b_1 = b_2$ and $\alpha_1 = \alpha_2$ by monotonicity and continuity of the transformation. Then, with α and b fixed, the map $G \mapsto F$ is strictly monotonic, implying $G_1 = G_2$, hence $\theta_1 = \theta_2$ by identifiability of the baseline. □

This result ensures that the parameters can be uniquely estimated from data, a prerequisite for meaningful inference.

3.4. Mode Analysis

The mode(s) of the TL-HT-G distribution satisfy $\frac{d}{dy}\log f(y) = 0$, that is:

$$\frac{g'(y;\theta)}{g(y;\theta)} + \frac{(2\alpha-1)(-g(y;\theta))}{\bar{G}(y;\theta)} + \frac{(b-1)\frac{d}{dy}D_G(y)}{D_G(y)} - \frac{(2\alpha+1)(1-\alpha)g(y;\theta)}{1-(1-\alpha)G(y;\theta)} = 0.$$

Unimodality occurs when this equation has exactly one solution. The number of modes can change at critical parameter values. For the special case of TL-HT-W (Weibull baseline), the mode equation reduces to:

$$\frac{\omega-1}{y} - \lambda\omega y^{\omega-1} - (2\alpha-1)\lambda\omega y^{\omega-1} + (b-1)\frac{d}{dy}\log D_A(y) - \frac{(2\alpha+1)(1-\alpha)\lambda\omega y^{\omega-1}e^{-\lambda y^{\omega}}}{1-(1-\alpha)(1-e^{-\lambda y^{\omega}})} = 0.$$

Result 1
For $\omega \geq 1$, the density is either unimodal or decreasing (reversed-J). For $\omega < 1$, a bathtub-shaped density may arise. This analytically supports the numerical shapes (density) shown in Figure 1.

3.5. Analytical Hazard Rate Shapes

The hrf shape is determined by the derivative of $\log h(y)$. The family can exhibit:

- **Monotone increasing:** When $\frac{d}{dy}\log h(y) > 0$ for all y. This occurs, for example, when $b \geq 1$, $\alpha \geq 1$, and the baseline hrf is increasing.
- **Monotone decreasing:** When $\frac{d}{dy}\log h(y) < 0$ for all y. This occurs, for example, when $0 < b < 1$, $0 < \alpha < 0.5$, and decreasing baseline hrf.
- **Bathtub (decreasing then increasing):** Requires the baseline hrf to be bathtub-shaped and parameters such that the transformation preserves the turning point.
- **Unimodal (increasing then decreasing):** Requires the baseline hrf to be unimodal, with b and α modulating the location of the turning point.

Proposition 3 (Hazard shape for TL-HT-W)
For the TL-HT-W distribution with Weibull baseline hrf $h_G(y) = \lambda\omega y^{\omega-1}$:

- If $\omega \geq 1$ and $\alpha b \geq 1$, the hrf is increasing.
- If $\omega \leq 1$ and $\alpha b \leq 1$, the hrf is decreasing.
- If $\omega > 1$ and $\alpha b < 1$, a bathtub shape may appear for intermediate parameter ranges.
- If $\omega < 1$ and $\alpha b > 1$, a unimodal (inverted bathtub) shape may appear.

These analytical conditions directly support the numerical hazard plots in Figures 1, 2, and 3, confirming that the observed shapes are not merely artifacts of specific parameter choices but inherent to the family's structure.

Table 1. Summary of Theoretical Properties of the TL-HT-G Family

Property	**Analytical Result**	**Key Parameter**
Near-zero behaviour	$f(y) \sim 2b\alpha^2 c_0 y^k$	Baseline shape k
Tail heaviness	$\bar{F}(y) \sim b\alpha^{-2\alpha}[\bar{G}(y)]^{2\alpha}$	α
Regular variation tail index	$2\alpha\xi$ (if baseline index ξ)	α
Identifiability	Unique parameters	b, α, θ
Unimodality condition	Depends on baseline and parameters	b, α, baseline shape
Increasing hazard (Weibull)	$\omega \geq 1,\ \alpha b \geq 1$	ω, α, b
Decreasing hazard (Weibull)	$\omega \leq 1,\ \alpha b \leq 1$	ω, α, b

4. Statistical Properties

This section covers a range of mathematical and statistical properties, including order statistics, complete and incomplete moments, and stochastic ordering.

4.1. Quantile Function

Inverting the TL-HT-G cdf gives the quantile function $(Q_Y(u))$ of the TL-HT-G FoDs, that is, solving the nonlinear equation presented in Equation (9):

$$\left[1 - \left(\frac{\bar{G}(Q_Y(u);\vartheta)}{1-(1-\alpha)G(Q_Y(u);\vartheta)}\right)^{2\alpha}\right]^b = u, \tag{9}$$

for $Q_Y(u)$, where $u \in (0,1)$. The TL-HT-G FoDs' quantile function is therefore given by

$$Q_Y(u) = G^{-1}\left[\frac{\left(1-u^{\frac{1}{b}}\right)^{\frac{1}{2\alpha}} - 1}{(1-\alpha)\left(1-u^{\frac{1}{b}}\right)^{\frac{1}{2\alpha}} - 1}\right]. \tag{10}$$

Accordingly, the quantile values can be obtained from Equation (10) by utilizing the R software to solve the nonlinear equation based on a given baseline cdf G(.). See **web appendix** for derivations.

4.2. Density Function Series Expansion

This subsection gives the TL-HT-G FoDs' density expansion. The pdf of the TL-HT-G FoDs can be expressed as Equation (11):

$$f(y;b,\alpha,\vartheta) \quad = \quad \sum_{j=0}^{\infty} \Phi_{j+1} g_{j+1}(y;\vartheta), \tag{11}$$

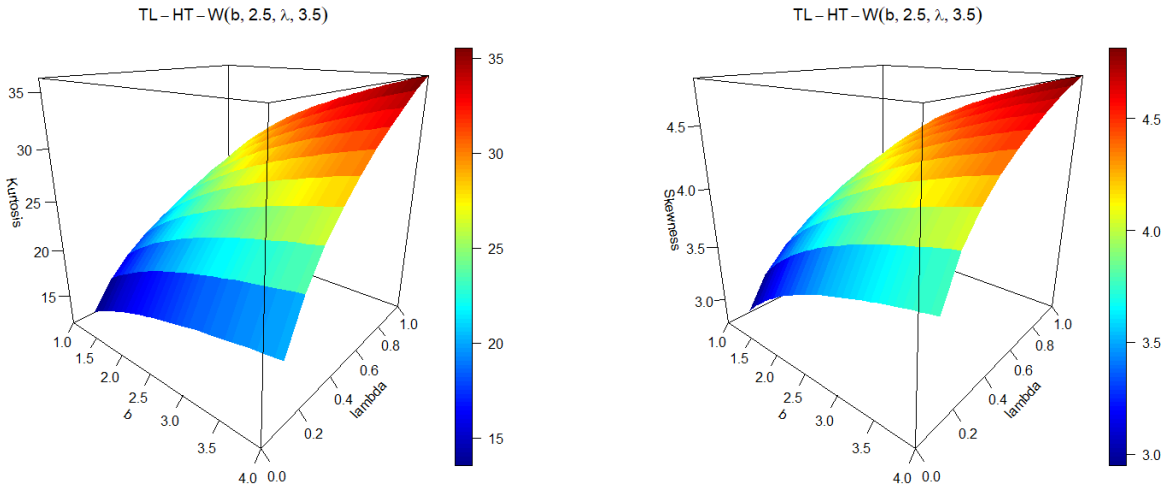

(a) **(b)**

Figure 4. TL-HT-W distribution's kurtosis (a) and skewness (b) in 3D plots

where $g_{j+1}(y;\vartheta) = (j+1)g(y;\vartheta)G^j(y;\vartheta)$ is the exponentiated-G (Expo-G) distribution with power parameter $(j+1)$ and Φ_{j+1} defines the linear component given by

$$\begin{aligned}\Phi_{j+1} &= \sum_{i,e,h=0}^{\infty} \frac{(-1)^{i+e+j}}{j+1} 2b\alpha^2 (1-\alpha)^h \binom{b-1}{e} \binom{h+2\alpha(e+1)}{h} \binom{h}{i} \\ &\times \binom{4\alpha(e+1)-2+i}{j}. \end{aligned} \tag{12}$$

Thus, the TL-HT-G FoDs can be represented as an infinite linear combination of Expo-G densities, from which various statistical properties, including order statistics, probability-weighted moments, and entropy, can be derived. The **web appendix** contains detailed derivations.

4.3. Moments

Suppose W_{j+1} represents an Expo-G distributed random variable (RV) with a power parameter $(j+1)$, in that case, the p^{th} moment of the TL-HT-G FoDs can be expressed as $E(Y^p) = \sum_{j=0}^{\infty} \Phi_{j+1} E(W_{j+1}^p)$, where $E(W_{j+1}^p)$ represents the p^{th} moment of W_{j+1}, and Φ_{j+1} is defined in Equation (12).

Additionally, the p^{th} incomplete moment can be derived as $I_Y(t) = \int_0^t y^p f(y)dy = \sum_{j=0}^{\infty} \Phi_{j+1} I_{j+1}(t;p,\vartheta)$, where $I_{j+1}(t;p,\vartheta) = \int_0^t y^p g_{j+1}(y;\vartheta)dy$ represents the incomplete moment of W_{j+1}. Furthermore, the moment generating function (mgf) of Y is $M_Y(t) = \sum_{j=0}^{\infty} \Phi_{j+1} E(e^{tW_{j+1}})$, where $E(e^{tW_{j+1}})$ represents the mgf of W_{j+1} and Φ_{j+1} is specified in Equation (12).

Incomplete moments play a pivotal role in the construction of Bonferroni curves and Lorenz curves, while complete moments are valuable in the computation of coefficients of variation, skewness, kurtosis, and other related characteristics.

Panels (a) and (b) in Figure [4] illustrate the increase in peakedness and skewness of the TL-HT-W distribution as parameters b and λ are increased, with α and γ held constant.

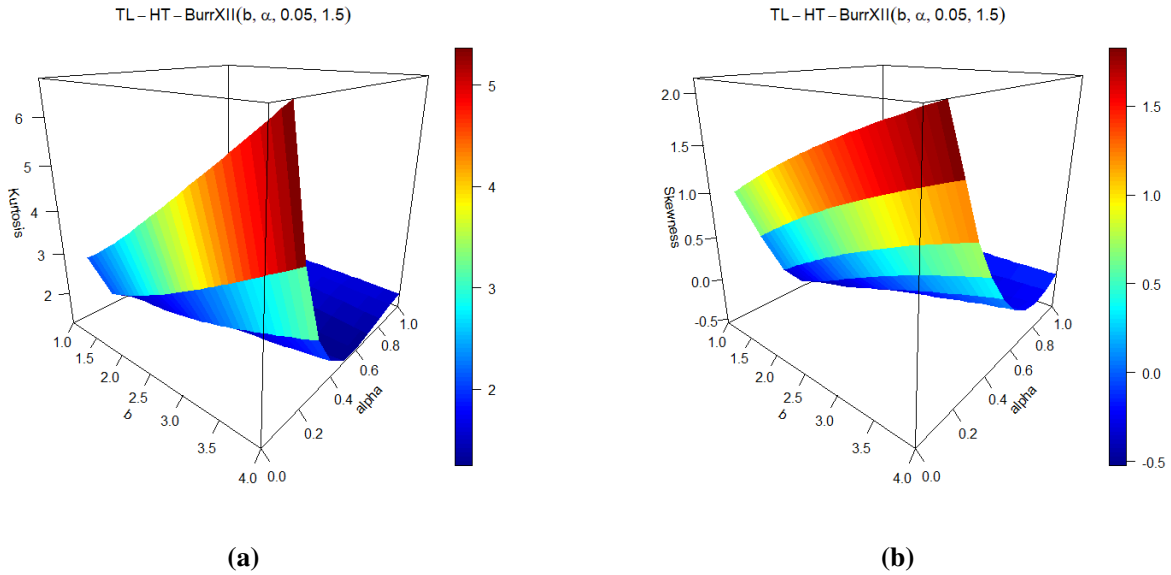

(a) **(b)**

Figure 5. TL-HT-Burr XII distribution's kurtosis (a) and skewness (b) depicted in 3D plots

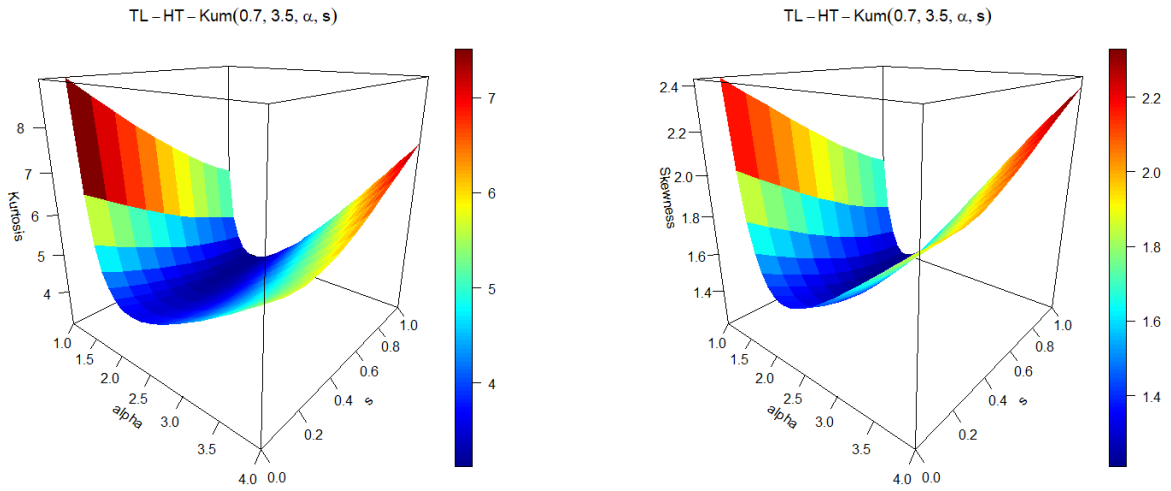

(a) **(b)**

Figure 6. TL-HT-Kum distribution's kurtosis (a) and skewness (b) depicted in 3D plots

Figure [5] shows that after controlling for c and k, various degrees of kurtosis (Figure [5] (a)) and skewness (Figure [5] (b)) for the TL-HT-Burr XII distribution are observed as b and α increase.
Figure [6] (a) and (b) shows that the TL-HT-Kum distribution exhibits different levels of kurtosis and skewness as α and s increase, while controlling for a and b.

4.4. Stochastic Ordering

Stochastic ordering is a concept employed to compare the relative magnitudes of RVs. Two commonly used stochastic orders are the likelihood ratio order (LRO) and the hazard rate order (HRO), which provide measures of the likelihood and hazard rate, respectively, to determine the superiority of one RV over another.

If we consider two variables W_1 and W_2 with cdfs $F_{W_1}(t)$ and $F_{W_2}(t)$, the survival functions of W_1 and W_2 are $\bar{F}_{W_1}(t) = 1 - F_{W_1}(t)$ and $\bar{F}_{W_2}(t) = 1 - F_{W_2}(t)$, respectively. If $\bar{F}_{W_1}(t) \leq \bar{F}_{W_2}(t)$ or $F_{W_1}(t) \geqslant F_{W_2}(t)$ $\forall t$, then the random variable W_1 is defined to be stochastically smaller than the random variable W_2, written as $W_1 <_{st} W_2$. The concepts of HRO and LRO possess greater strength and are characterized by $W_1 <_{hr} W_2$ if $h_{W_1}(t) \geqslant h_{W_2}(t)$ $\forall t$, and $W_1 <_{lr} W_2$ if $\frac{h_{W_1}(t)}{h_{W_2}(t)}$ is decreasing in t. Note that, $W_1 <_{lr} W_2 \Rightarrow W_1 <_{hr} W_2 \Rightarrow W_1 <_{st} W_2$. See Shaked and Shanthikumar [21] for additional details.

Theorem 1
Let W_1 and W_2 be independent RVs such that $W_1 \sim TL-HT-G(\alpha, b_1, \vartheta)$ and $W_2 \sim TL-HT-G(\alpha, b_2, \vartheta)$ distributions. If $b_1 < b_2$, then W_1 and W_2 are stochastically ordered.

Proof
The pdfs of W_1 and W_2 are:

$$f_1(y) = f_1(y; b_1, \alpha, \vartheta) = 2b_1\alpha^2 \left[D_G(y;\alpha,\vartheta)\right]^{b_1-1} \frac{g(y;\vartheta)\left\{\bar{G}(y;\vartheta)\right\}^{2\alpha-1}}{\left\{1-(1-\alpha)G(y;\vartheta)\right\}^{2\alpha+1}},$$

and

$$f_2(y) = f_2(y; b_2, \alpha, \vartheta) = 2b_2\alpha^2 \left[D_G(y;\alpha,\vartheta)\right]^{b_2-1} \frac{g(y;\vartheta)\left\{\bar{G}(y;\vartheta)\right\}^{2\alpha-1}}{\left\{1-(1-\alpha)G(y;\vartheta)\right\}^{2\alpha+1}}.$$

The ratio

$$\frac{f_1(y)}{f_2(y)} = \frac{b_1}{b_2}\left[D_G(y;\alpha,\vartheta)\right]^{b_1-b_2}. \tag{13}$$

Taking the derivative of Equation (13) with respect to y, we obtain

$$\frac{\partial}{\partial y}\left(\frac{f_1(y)}{f_2(y)}\right) = \frac{b_1}{b_2}(b_1-b_2)\left[D_G(y;\alpha,\vartheta)\right]^{b_1-b_2-1}\frac{\partial}{\partial y}\left(\frac{\bar{G}(y;\vartheta)}{1-(1-\alpha)G(y;\vartheta)}\right)^{2\alpha}.$$

Now if $b_1 < b_2$, then $\frac{\partial}{\partial y}\left(\frac{f_1(y)}{f_2(y)}\right) < 0$. Therefore, the likelihood ratio order $W_1 <_{lr} W_2$ exists. Consequently, the RVs W_1 and W_2 are stochastically ordered. □

5. Estimation

This section focuses on estimating the unknown parameters of the TL-HT-G FoDs using five different techniques: maximum likelihood estimation (MLE), Cramér-von Mises (CVM) minimum distance, ordinary least squares (OLS), weighted least squares (WLS), and Anderson-Darling (AD). In our estimation, we will employ the Newton-Raphson method due to its rapid convergence and efficiency in solving nonlinear equations, which proves particularly beneficial for applications related to root finding and optimization.

5.1. MLE Technique

This subsection presents MLEs for the TL-HT-G FoDs considering both complete and censored data.

5.1.1. Estimation without Censoring Consider a random sample of size n, where each observation, Y_i, follows the TL-HT-G distribution, and let $\Lambda = (\alpha, b, \vartheta)^T$ represent the vector of model parameters. The log-likelihood function $\ell = \ell(\Lambda)$ for this sample is

$$\begin{aligned}\ell = \ell(\Lambda) &= 2n\ln(\alpha) + n\ln(2b) + (b-1)\sum_{i=1}^{n}\ln\left[D_G(y;\alpha,\vartheta)\right] + \sum_{i=1}^{n}\ln[g(y_i;\vartheta)] \\ &+ (2\alpha-1)\sum_{i=1}^{n}\ln\left(1-G(y_i;\vartheta)\right) - (2\alpha+1)\sum_{i=1}^{n}\ln\left[1-(1-\alpha)G(y;\vartheta)\right]^{2\alpha+1}. \end{aligned} \tag{14}$$

The numerical computation of the nonlinear equation $\left[\frac{\partial\ell}{\partial\alpha}, \frac{\partial\ell}{\partial b}, \frac{\partial\ell}{\partial\vartheta_k}\right]^T = \mathbf{0}$ utilizing R statistical software generates the MLEs of the parameters α, b and ϑ_k. The **web appendix** contains the explicit expressions of the log-likelihood function partial derivatives with respect to each individual element of the parameter vector.

5.1.2. Estimation with Censoring Survival time studies frequently produce censored observations, implying that there are partial observations during the specified time interval. We shall use type I censoring, a predominant form of right censoring commonly observed in the field of survival analysis.

Let us consider a study comprising a random sample of n patients, where each patient has an independent censoring time denoted as W_k (for $k = 1, 2, 3, ..., n$). In other words, W_k represents the time interval between the entry of the patient into the study and the termination of the study. Additionally, let Y_k also represent the failure time of the k^{th} patient. The variables Y_k and W_k are considered to be independent and are assumed to follow the distribution of the TL-HT-G FoDs. For $T_k = min(Y_k, W_k), (T_k, \rho_k)$, ρ_k takes the value of 0 if censoring occurs and 1 if failure is observed. As a result, the log-likelihood function ℓ can be formulated in the following manner:

$$\ell = \sum_{k=1}^{n}\rho_k\log\left(f(t_k)\right) + \sum_{k=1}^{n}(1-\rho_k)\log\left(S(t_k)\right), \tag{15}$$

where $S(.)$ and $f(.)$ are defined in Equation (6) and Equation (7), respectively. The MLEs can be numerically obtained by maximizing the log-likelihood function described in Equation (15).

5.2. CVM, OLS, WLS and AD Estimation

Let $Y_{1:n} \leq Y_{2:n} \leq Y_{3:n} ..... \leq Y_{n:n}$ be order statistics of a random sample of size n obtained from the TL-HT-G FoDs. We deduce the following estimations:

- The CVM estimates $\hat{b}_{CVM}, \hat{\alpha}_{CVM}$ and $\hat{\vartheta}_{CVM}$ of the TL-HT-G FoDs vector of parameters are found by minimizing the function

$$S_{CVM}(b,\alpha,\vartheta) = \frac{1}{12n} + \frac{1}{n}\sum_{i=1}^{n}\left(\left[D_G(y;\alpha,\vartheta)\right]^b - \frac{2i-1}{2n}\right)^2.$$

  with respect to $b, \alpha,$ and ϑ. Estimates of the TL-HT-G FoDs are obtained by solving a set of nonlinear equations as follows:

$$\sum_{i=1}^{n}\left(\left[D_G(y;\alpha,\vartheta)\right]^b - \frac{2i-1}{2n}\right)^2 \Delta_t\left(y_{(i)};\alpha,b,\vartheta\right) = 0$$

  for t=1,2,3, where

$$\Delta_1\left(y_{(i)};b,\alpha,\vartheta\right) = \frac{\partial}{\partial b}\left[D_G(y;\alpha,\vartheta)\right]^b, \tag{16}$$

$$\Delta_2\left(y_{(i)};b,\alpha,\vartheta\right)=\frac{\partial}{\partial\alpha}\left[D_G(y;\alpha,\vartheta)\right]^b, \tag{17}$$

and

$$\Delta_{3,k}\left(y_{(i)};b,\alpha,\vartheta\right)=\frac{\partial}{\partial\vartheta,j}\left[D_G(y;\alpha,\vartheta)\right]^b, \tag{18}$$

for $k=1,2,....,p$. Note that p is the number of parameters in the vector ϑ.

- The OLS estimates of b,α and ϑ (denoted by $\hat{b}_{OLS},\hat{\alpha}_{OLS}$ and $\hat{\vartheta}_{OLS}$) of the TL-HT-G FoDs are found by minimizing the function

$$\begin{aligned} S_{OLS}(b,\alpha,\vartheta) &= \frac{1}{12n}+\frac{1}{n}\sum_{i=1}^{n}\left(F(y_{(i)}|b,\alpha,\vartheta)-\frac{i}{n+1}\right)^2 \\ &= \frac{1}{12n}+\frac{1}{n}\sum_{i=1}^{n}\left(\left[D_G(y;\alpha,\vartheta)\right]^b-\frac{i}{n+1}\right)^2, \end{aligned} \tag{19}$$

with respect to b,α, and ϑ. Estimates of the TL-HT-G FoDs are found by solving the following set of nonlinear equations:

$$\sum_{i=1}^{n}\left(\left[D_G(y;\alpha,\vartheta)\right]^b-\frac{i}{n+1}\right)^2\Delta_t\left(y_{(i)};b,\alpha,\vartheta\right)=0$$

where $\Delta_t\left(y_{(i)};b,\alpha,\vartheta\right)$ is specified by Equations (16), (17) and (18).

- Weighted least squares (WLS) is preferred over OLS as it effectively addresses heteroscedasticity, improving estimation efficiency and robustness to outliers, while ensuring valid statistical inferences Usman et al. [22]. WLS estimates of b,α, and ϑ denoted by $\hat{b}_{WLS},\hat{\alpha}_{WLS}$, and $\hat{\vartheta}_{WLS}$ from the TL-HT-G FoDs can be obtained by minimizing the function

$$\begin{aligned} S_{WLS}(b,\alpha,\vartheta) &= \sum_{i=1}^{n}\frac{(n+1)^2(n+2)}{i(n-i+1)}\left(F(y_{(i)}|\alpha,b,\vartheta)-\frac{i}{n+1}\right)^2 \\ &= \sum_{i=1}^{n}\frac{(n+1)^2(n+2)}{i(n-i+1)}\left(\left[W(y;\alpha,\vartheta)\right]^b-\frac{i}{n+1}\right)^2 \end{aligned} \tag{20}$$

with respect to b,α and ϑ. Estimates of the TL-HT-G FoDs are then found through the resolution of a system of nonlinear equations:

$$\sum_{i=1}^{n}\frac{(n+1)^2(n+2)}{i(n-i+1)}\left(\left[D_G(y;\alpha,\vartheta)\right]^b-\frac{i}{n+1}\right)^2\Delta_t\left(y_{(i)};b,\alpha,\vartheta\right)=0,$$

where $\Delta_t\left(y_{(i)};b,\alpha,\vartheta\right)$ is specified by Equations (16), (17) and (18).

- The AD estimates of b,α, and ϑ of the TL-HT-G FoDs parameters denoted by $\hat{b}_{AD},\hat{\alpha}_{AD}$ and $\hat{\vartheta}_{AD}$ are found by minimizing the function in Equation (21):

$$\begin{aligned} A^2 &= \frac{1-n^2}{n}+\sum_{i=1}^{n}\left[(2i-1)\log\left(F(y_{(i)}|b,\alpha,\vartheta)\right)\right] \\ &- \sum_{i=1}^{n}\left[2(n-i)+1\right)\log(S(y_{(i)}|b,\alpha,\vartheta))\Big] \end{aligned} \tag{21}$$

with respect to b, α, and ϑ, where $F(.)$ and $S(.)$ are defined by Equations (5) and (6). An alternative approach involves solving the following system of nonlinear equations:

$$\sum_{i=1}^{n}(2i-1)\left[\frac{\Delta_t\left(y_{(i)};b,\alpha,\vartheta\right)}{F(y_{(i)}|b,\alpha,\vartheta)}-\frac{\Delta_t\left(y_{(i)};b,\alpha,\vartheta\right)}{S(y_{(i)}|b,\alpha,\vartheta)}\right]=0,$$

where $\Delta_t\left(y_{(i)};b,\alpha,\vartheta\right)$ is specified by Equations (16), (17) and (18).

6. Risk Measures

Risk measures can be defined as tools that actuaries employ to assess market risk. The following risk measures are studied in this section.

6.1. Value at Risk

Value at Risk (VaR) measures the potential financial losses that a firm, portfolio, or position may experience within a defined time period. VaR_q for the TL-HT-G FoDs is calculated from Equation (22):

$$Y_q = G^{-1}\left[\frac{\left(1-q^{\frac{1}{b}}\right)^{\frac{1}{2\alpha}}-1}{(1-\alpha)\left(1-q^{\frac{1}{b}}\right)^{\frac{1}{2\alpha}}-1}\right], \tag{22}$$

for $b,\alpha>0$, $q\in(0,1)$ represents the significance level and $G(.)$ is the baseline cdf.

6.2. Tail Value at Risk

Tail Value at Risk (TVaR) quantifies the anticipated magnitude of losses in the scenario where an outcome surpassing a predetermined probability threshold materializes. The TVaR for the TL-HT-G FoDs is given by Equation (23):

$$TVaR_q = E\left(Y|Y>y_q\right)=\frac{1}{1-q}\sum_{j=0}^{\infty}\int_{VaR_q}^{\infty}y\Phi_{j+1}g_{j+1}(y;\vartheta)dy, \tag{23}$$

where Φ_{j+1} is as defined by Equation (12) and $g_{j+1}(y;\vartheta)=G^j(y;\vartheta)g(y;\vartheta)(j+1)$ is the Expo-G pdf with power parameter $(j+1)$.

6.3. Tail Variance

Tail Variance (TV_q) measures the conditional variance of losses under the assumption that they exceed the Value at Risk (VaR) with a probability threshold p. Equation (24) provides the expression for the TV_q of the TL-HT-G FoDs:

$$\begin{aligned}TV_q &= E\left(Y^2\mid Y>y_q\right)-\left(TVaR_q\right)^2\\ &= \frac{1}{1-q}\int_{VaR_q}^{\infty}y^2f(y)dy-\left(TVaR_q\right)^2\\ &= \frac{1}{1-q}\sum_{j=0}^{\infty}\Phi_{j+1}\int_{VaR_q}^{\infty}y^2g_{j+1}(y;\vartheta)dy-\left(TVaR_q\right)^2,\end{aligned} \tag{24}$$

where $g_{j+1}(y;\vartheta)=G^j(y;\vartheta)g(y;\vartheta)(j+1)$ is the Expo-G distribution with a power parameter $(j+1)$, ϑ denotes the parameter vector and Φ_{j+1} is as stated by (12).

6.4. Tail Variance Premium (TVaP)

Risk professionals are concerned about risks exceeding certain thresholds. Such conditions are common in insurance, for example, in policies involving deductibles and reinsurance contracts. Tail variance premium answers demands to these circumstances. The TVaP of the TL-HT-G FoDs is expressed as

$$TVaP_q = TVaR_q + \theta(TV_q), \tag{25}$$

where $0 < \theta < 1$ is a risk aversion parameter.

6.5. Risk Measures Numerical Study

We provide a comprehensive analysis using numerical simulations to evaluate risk metrics. The risk measures of the TL-HT-W distribution are compared to the Kumaraswamy-Weibull (KW), type-I heavy-tailed Weibull (TI-HT-W), and the standard Weibull distributions.

To ensure accurate estimations across different distributions, the simulation results are obtained by randomly generating samples of size $n = 100$ from the specified distributions and estimating the parameters using the MLE technique. The calculations are iteratively performed 1,000 times to enhance precision in the estimations across the various distributions.

However, a direct comparison of raw risk measure values across distributions can be misleading, as differences may arise from scale effects rather than intrinsic tail behavior. To address this, we employ a standardization procedure that removes location and scale effects, isolating pure tail behavior. For each distribution, we:

1. Estimate parameters via MLE from samples of size $n = 100$ (repeated 1,000 times);
2. Compute the scale-normalization factor $c = 1/Q_{0.5}(Y)$, where $Q_{0.5}(Y)$ is the median;
3. Compute standardized risk measures:

$$\text{VaR}_q^{\text{std}} = c\text{VaR}_q, \quad \text{TVaR}_q^{\text{std}} = c\text{TVaR}_q, \quad \text{TV}_q^{\text{std}} = c^2\text{TV}_q;$$

4. Compare standardized values across distributions.

We also compute scale-invariant tail ratios:

$$\text{Tail Ratio}_q = \frac{\text{TVaR}_q}{\text{VaR}_q}$$

and

$$\text{Excess Ratio}_q = \frac{\text{TVaR}_q - \text{VaR}_q}{\text{VaR}_q},$$

which provide direct measures of tail behavior that are independent of scale.

Table 2 displays the outcomes of the numerical simulations, presenting both the raw estimated risk measures and the derived standardized metrics for the four heavy-tailed distributions under consideration.

To facilitate a meaningful comparison of tail heaviness independent of scale, Table 3 presents the standardized risk measures (normalized to a common median of 1) and the scale-invariant tail ratios for each distribution at the extreme quantiles.

Interpretation: The raw risk measures in Table 2 show that the TL-HT-W distribution yields consistently higher VaR, TVaR, TV, and TVaP values compared to the competing distributions across all quantile levels. However, as noted earlier, these raw comparisons may be confounded by scale differences. After standardizing to a common median (Table 3), the TL-HT-W distribution continues to exhibit the largest standardized VaR and TV values at the 95% quantile, confirming its substantial tail heaviness relative to the KW and Weibull distributions. The TI-HT-W shows comparable tail ratios, but the TL-HT-W maintains more consistent heavy-tail behavior across quantile levels, with its tail ratio remaining above 0.80 at both the 95% and 99% levels. The Weibull distribution exhibits the largest tail ratio; however, this is accompanied by very small TV values, indicating a fundamentally different

Table 2. Numerical Simulations Results for the Actuarial Risk Measures

Model	Risk Metric	0.75	0.8	0.85	0.9	0.95	0.99
TL-HT-W($b = 1.1, \alpha = 0.6, \lambda = 0.5, \omega = 2.3$)	VaR	5.1647	6.1345	6.6740	7.6124	8.2214	10.2131
	TVaR	3.9807	5.2243	6.2134	6.8654	6.9087	8.4586
	TV	6.2214	7.0914	7.7002	7.9991	8.5134	9.1648
	TVaP	9.4679	11.1457	13.1445	15.2231	16.8574	19.1457
KW($a = 1.2, b = 1.1, \alpha = 0.6, \beta = 1.5$)	VaR	0.7120	0.8024	0.9124	0.9945	1.2353	1.6610
	TVaR	1.1918	1.3001	1.4344	1.7610	1.8623	2.3021
	TV	1.2441	1.4920	1.5187	1.6363	1.7512	1.9712
	TVaP	1.5178	1.5941	1.7534	1.9556	2.2359	2.7071
TI-HT-W($\alpha = 0.6, \lambda = 0.5, \omega = 2.3$)	VaR	0.6712	0.9871	0.9722	1.3412	1.9745	3.0548
	TVaR	1.5614	2.0073	2.6701	2.9934	3.4218	4.3497
	TV	2.1647	4.4554	4.4316	4.6784	6.1237	7.164
	TVaP	4.6187	5.2146	5.87241	6.8105	8.1647	8.4161
Weibull($\lambda = 0.5, \omega = 2.3$)	VaR	0.5759	0.6141	0.6593	0.7167	0.8030	0.9669
	TVaR	0.1776	01269	0.0672	0.0227	0.0063	0.0009
	TV	0.3949	0.4707	0.5686	0.6795	0.8204	1.1106
	TVaP	0.4738	0.5034	0.5005	0.6327	0.7856	1.0995

Table 3. Standardized Actuarial Risk Measures and Tail Ratios

Model	c	Standardized Measures			Tail Ratios	
		$\text{VaR}_{0.95}^{\text{std}}$	$\text{TVaR}_{0.95}^{\text{std}}$	$\text{TV}_{0.95}^{\text{std}}$	$\text{Ratio}_{0.95}$	$\text{Ratio}_{0.99}$
TL-HT-W	0.1936	1.592	1.338	1.647	0.840	0.828
KW	0.0594	1.001	0.073	0.104	0.073	0.099
TI-HT-W	0.4472	1.000	0.883	0.869	0.883	0.987
Weibull	0.1633	1.000	1.333	0.162	1.333	1.341

tail structure characterized by rapid decay beyond the VaR threshold. These results demonstrate that the TL-HT-W distribution is particularly well-suited for modeling heavy-tailed data in actuarial applications, with tail behavior that is intrinsically controlled by the parameter α (see Section 3.2, Corollary 1). A model with higher standardized risk measure values is considered to have a more pronounced heavy tail, conditional on scale. Hence, we conclude that the TL-HT-W has genuinely heavier tails than the KW and Weibull distributions, while being competitive with the TI-HT-W, making it appropriate for modeling heavy-tailed data in actuarial risk management.

7. Simulations

In this section, the properties of the parameter estimators of the TL-HT-W distribution are analyzed using Monte Carlo simulation in R. To ensure statistical reliability, we conducted multiple iterations of the estimation procedure, closely monitoring convergence through diagnostic plots. The correctness of the estimates was evaluated by calculating average bias (AVBIAS) and root mean square error (RMSE), where AVBIAS indicates the average deviation between the estimated values and the true parameters. The quantile function specified in (10) was utilized to generate stochastic samples from the TL-HT-W distribution. Tables [4] and [5] show the average bias (AVBIAS) and the root mean square error (RMSE) of the CVM, MLE, OLS, WLS and AD estimators for various parameter values. The AVBIAS and RMSE for an estimated parameter, say ($\hat{\lambda}$), are calculated as follows:

AVBIAS($\hat{\lambda}$) = $\frac{\sum_{i=1}^{N} \hat{\lambda}_i}{N}$ - λ and, RMSE($\hat{\lambda}$) = $\sqrt{\frac{\sum_{i=1}^{N} (\hat{\lambda}_i - \lambda)^2}{N}}$, respectively.

Three thousand (N = 3000) replications with sample sizes $(n) = 25, 50, 100, 200, 400$, and 800 and initial parameter values $(b, \alpha, \lambda, \omega) = (0.8, 0.8, 1.5, 2.2)$ and
$(b, \alpha, \lambda, \omega) = (0.2, 0.3, 0.2, 2.4)$ were utilized in the simulation experiments.

Tables [4] and [5] include a row labeled, Sum of Ranks, which represents the partial sum of the ranks. The subscript (in parenthesis) next to each estimator indicates its rank for a specific metric. For instance, in Table [4], the RMSE of $\hat{\alpha}$ obtained through the CVM method is shown as $1.1583_{(4)}$ for $n = 25$. This means that the CVM method ranks fourth among all other estimators in terms of RMSE of $\hat{\alpha}$. Therefore, when n = 25, the CVM method exhibits the fourth-best RMSE of $\hat{\alpha}$ compared to all other estimators. Furthermore, the AVBIAS of $\hat{\lambda}$ derived by the MLE approach is $0.5616_{(2)}$ for $n = 50$, signifying the second best AVBIAS of $\hat{\lambda}$ when compared to other estimators. Table [6] presents the partial and total ranks assigned to the estimation techniques employed in estimating the TL-HT-W distribution across different model parameter values. Figures 7 (a–d) and 8 (a–d) illustrate the monotonic decrease in RMSEs for the estimated parameters as the sample size increases, across all four estimation techniques.

Table 4. Simulations Results for the Various Estimation Methods for $b = 0.8, \alpha = 0.8, \lambda = 1.5, \omega = 2.2$

		MLE		CVM		OLS		WLS		AD	
n	Parameters	RMSE	AVBIAS	RMSE	AVBIAS	RMSE	AVBIAS	RMSE	AVBIAS	RMSE	AVBIAS
25	b	$0.8395_{(4)}$	$0.5719_{(1)}$	$0.9265_{(5)}$	$0.8324_{(5)}$	$0.7836_{(2)}$	$0.6454_{(4)}$	$0.8181_{(3)}$	$0.6177_{(3)}$	$0.6933_{(1)}$	$0.5824_{(2)}$
	α	$1.2051_{(5)}$	$0.5175_{(1)}$	$1.1583_{(4)}$	$0.9124_{(5)}$	$1.0568_{(3)}$	$0.8908_{(4)}$	$0.9249_{(2)}$	$0.7271_{(3)}$	$0.7133_{(1)}$	$0.6019_{(2)}$
	λ	$0.9132_{(5)}$	$0.6618_{(2)}$	$1.2511_{(4)}$	$0.9237_{(5)}$	$0.8454_{(1)}$	$0.3429_{(1)}$	$0.9623_{(2)}$	$0.6929_{(3)}$	$1.0376_{(3)}$	$0.9028_{(4)}$
	ω	$1.7269_{(4)}$	$0.9348_{(3)}$	$1.9746_{(5)}$	$0.9583_{(4)}$	$1.1939_{(1)}$	$0.8526_{(1)}$	$1.7055_{(3)}$	$0.9247_{(2)}$	$1.5068_{(2)}$	$1.0249_{(5)}$
	Sum of ranks		25		37		17		21		20
50	b	$0.7291_{(3)}$	$0.4647_{(1)}$	$0.7152_{(2)}$	$0.7127_{(5)}$	$0.6575_{(1)}$	$0.5822_{(2)}$	$0.7664_{(5)}$	$0.5971_{(3)}$	$0.7461_{(4)}$	$0.6909_{(4)}$
	α	$0.8122_{(2)}$	$0.2350_{(1)}$	$0.9521_{(5)}$	$0.7521_{(4)}$	$0.8992_{(4)}$	$0.8349_{(5)}$	$0.8343_{(3)}$	$0.6929_{(3)}$	$0.7322_{(1)}$	$0.6299_{(2)}$
	λ	$1.2032_{(5)}$	$0.5616_{(2)}$	$0.9603_{(4)}$	$0.7629_{(5)}$	$0.8152_{(2)}$	$0.3122_{(1)}$	$0.8179_{(3)}$	$0.6247_{(3)}$	$0.7240_{(1)}$	$0.6654_{(4)}$
	ω	$0.2847_{(1)}$	$0.6842_{(1)}$	$1.6934_{(5)}$	$0.9438_{(5)}$	$0.9736_{(2)}$	$0.8321_{(2)}$	$1.6266_{(4)}$	$0.9048_{(3)}$	$1.0788_{(3)}$	$0.9234_{(4)}$
	Sum of ranks		16		35		19		27		21
100	b	$0.6132_{(3)}$	$0.3929_{(1)}$	$0.7946_{(5)}$	$0.7522_{(5)}$	$0.5536_{(1)}$	$0.4744_{(2)}$	$0.7240_{(4)}$	$0.5249_{(3)}$	$0.5681_{(3)}$	$0.5254_{(4)}$
	α	$0.4526_{(1)}$	$0.1919_{(1)}$	$0.8646_{(5)}$	$0.6822_{(4)}$	$0.7675_{(4)}$	$0.7912_{(5)}$	$0.6847_{(3)}$	$0.5841_{(3)}$	$0.5687_{(2)}$	$0.4049_{(2)}$
	λ	$0.8738_{(5)}$	$0.4598_{(2)}$	$0.8030_{(4)}$	$0.6021_{(4)}$	$0.7717_{(2)}$	$0.2705_{(1)}$	$0.7823_{(3)}$	$0.6009_{(3)}$	$0.7541_{(1)}$	$0.784_{(5)}$
	ω	$0.8646_{(3)}$	$0.5238_{(1)}$	$1.0121_{(5)}$	$0.8723_{(5)}$	$0.8131_{(1)}$	$0.7633_{(3)}$	$0.9505_{(4)}$	$0.7928_{(4)}$	$0.8329_{(2)}$	$0.7522_{(2)}$
	Sum of ranks		17		37		19		27		21
200	b	$0.2413_{(1)}$	$0.1545_{(5)}$	$0.5113_{(4)}$	$0.5277_{(3)}$	$0.5029_{(3)}$	$0.4321_{(2)}$	$0.4998_{(2)}$	$0.2973_{(1)}$	$0.5789_{(5)}$	$0.5311_{(4)}$
	α	$0.3633_{(1)}$	$0.1505_{(1)}$	$0.8827_{(5)}$	$0.7011_{(5)}$	$0.5440_{(3)}$	$0.6824_{(4)}$	$0.3824_{2)}$	$0.4056_{(2)}$	$0.5886_{(4)}$	$0.4250_{(3)}$
	λ	$0.6685_{(3)}$	$0.4135_{(3)}$	$0.7772_{(5)}$	$0.5427_{(5)}$	$0.5451_{(1)}$	$0.2014_{(1)}$	$0.6870_{(4)}$	$0.5129_{(4)}$	$0.5829_{(4)}$	$0.3001_{(2)}$
	ω	$0.5820_{(1)}$	$0.3021_{(1)}$	$0.9042_{(5)}$	$0.4723_{(2)}$	$0.8342_{(2)}$	$0.7801_{(5)}$	$0.8442_{(4)}$	$0.5091_{(3)}$	$0.8424_{(3)}$	$0.7601_{(4)}$
	Sum of ranks		16		34		21		22		29
400	b	$0.1929_{(1)}$	$0.1208_{(1)}$	$0.2813_{(2)}$	$0.2614_{(3)}$	$0.3209_{(3)}$	$0.3327_{(4)}$	$0.3214_{(4)}$	$0.2104_{(2)}$	$0.4738_{(5)}$	$0.14821_{(5)}$
	α	$0.2150_{(1)}$	$0.1256_{(1)}$	$0.4489_{(4)}$	$0.3021_{(3)}$	$0.3372_{(3)}$	$0.3221_{(4)}$	$0.2684_{(2)}$	$0.1684_{(2)}$	$0.4622_{(5)}$	$0.3943_{(5)}$
	λ	$0.2937_{(1)}$	$0.1435_{(1)}$	$0.3462_{(2)}$	$0.2714_{(3)}$	$0.4790_{(5)}$	$0.1821_{(2)}$	$0.4764_{(4)}$	$0.3479_{(5)}$	$0.4723_{(3)}$	$0.2736_{(4)}$
	ω	$0.4601_{(3)}$	$0.2241_{(2)}$	$0.5602_{(4)}$	$0.2006_{(1)}$	$0.2234_{(1)}$	$0.2349_{(3)}$	$0.7036_{(5)}$	$0.3927_{(5)}$	$0.4417_{(2)}$	$0.3214_{(4)}$
	Sum of ranks		11		22		25		29		33
800	b	$0.1295_{(2)}$	$0.0804_{(2)}$	$0.1302_{(3)}$	$0.1119_{(3)}$	$0.0577_{(1)}$	$0.0124_{(1)}$	$0.3171_{(4)}$	$0.1984_{(4)}$	$0.3199_{(5)}$	$0.3077_{(5)}$
	α	$0.1027_{(1)}$	$0.1018_{(3)}$	$0.2474_{(4)}$	$0.1547_{(4)}$	$0.1083_{(2)}$	$0.1009_{(2)}$	$0.1677_{(3)}$	$0.0828_{(1)}$	$0.3107_{(5)}$	$0.2175_{(5)}$
	λ	$0.0715_{(1)}$	$0.0799_{(1)}$	$0.2842_{(4)}$	$0.1193_{(3)}$	$0.2242_{(3)}$	$0.1011_{(2)}$	$0.3965_{(5)}$	$0.2602_{(5)}$	$0.2241_{(2)}$	$0.1843_{(4)}$
	ω	$0.2814_{(2)}$	$0.1112_{(1)}$	$0.4715_{(4)}$	$0.1328_{(4)}$	$0.1994_{(1)}$	$0.1927_{(3)}$	$0.5340_{5)}$	$0.2041_{(4)}$	$0.3739_{(3)}$	$0.2118_{(5)}$
	Sum of ranks		13		29		15		31		34

Based on the findings presented in Tables [4] and [5], the following conclusions can be drawn:

i) Despite the large sample sizes of 400 and 800, the accuracy of MLE for the second parameter set may not have improved due to factors such as model convergence issues.
ii) TL-HT-W distribution exhibited stability, as indicated by the modest values of AVBIAS and RMSE for its four parameters.
iii) Both RMSE and AVBIAS generally decreased with increasing sample sizes across all estimation methods.
iv) Reliable estimations were achieved across all estimation methods, particularly when larger sample sizes were employed.

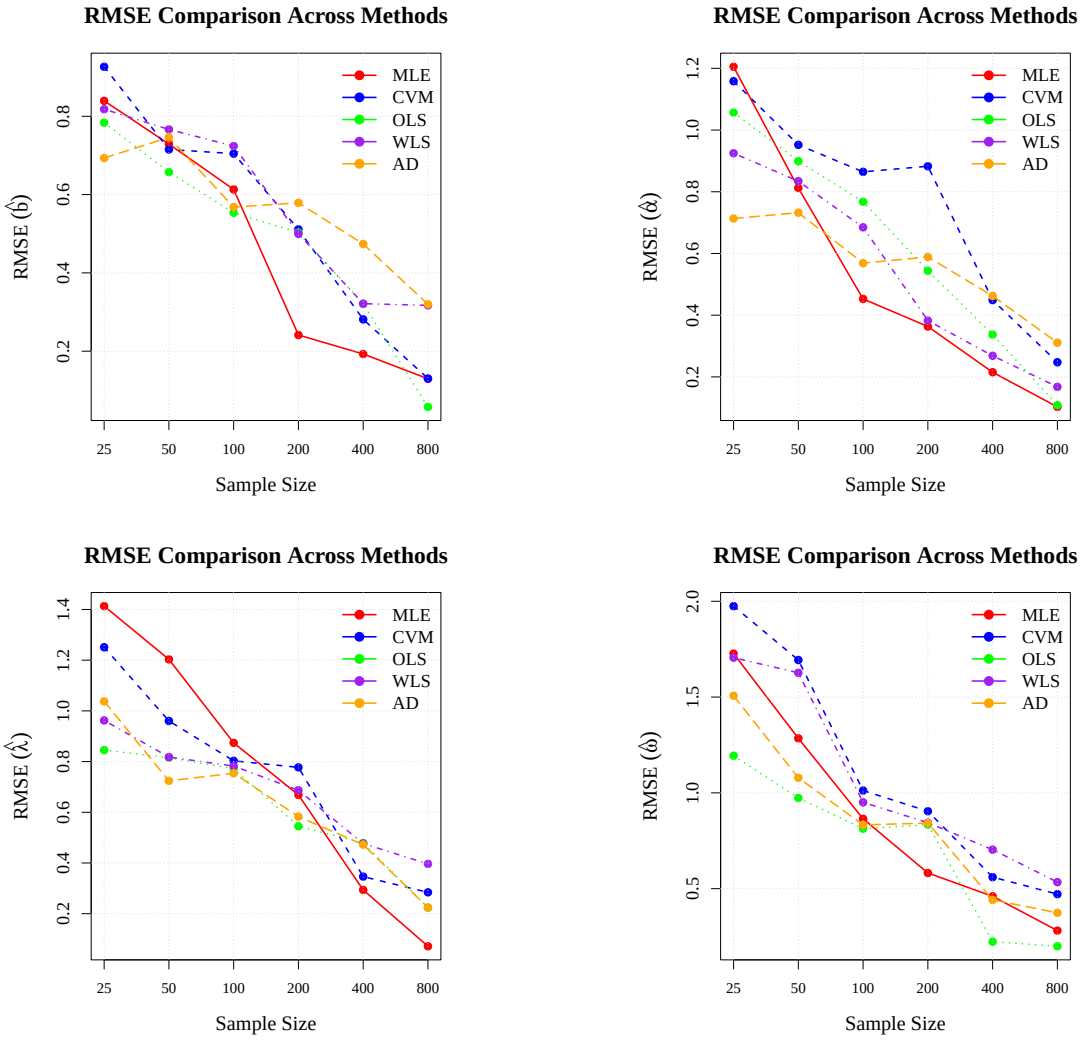

Figure 7. Plots of RMSEs for estimation of TL-HT-W distribution parameters for $b = 0.8, \alpha = 0.8, \lambda = 1.5, \omega = 2.2$, respectively.

Table [6] demonstrates that the MLE, followed by OLS, emerged as the most effective techniques in providing accurate estimates for the TL-HT-W distribution parameters. Consequently, we proceeded to estimate the TL-HT-W distribution's unknown parameters using the MLE technique.

To ensure that MLE's superior performance was not an artifact of the chosen optimization algorithm or starting values, we conducted robustness checks using three algorithms (Newton-Raphson/BFGS, Nelder-Mead, and simulated annealing) combined with three starting value strategies: true values, random perturbations ($\pm 20\%$), and uniform draws from plausible ranges. Convergence was declared when the relative change in log-likelihood fell below 10^{-8}. Across all 3,000 replications and sample sizes, parameter estimates and ranks were virtually identical regardless of algorithm or starting strategy, with non-convergence rates below 0.5% for Newton-Raphson and Nelder-Mead (rising to approximately 3% for simulated annealing at $n = 25$). Consequently, the recommendation of MLE is robust to algorithmic choices. We therefore report results from Newton-Raphson with true-value starts for consistency and computational efficiency.

Table 5. Simulations Results for Various Estimation Methods for $b = 0.2, \alpha = 0.3, \lambda = 0.2, \omega = 2.4$

		MLE		CVM		OLS		WLS		AD	
n	Parameters	RMSE	AVBIAS	RMSE	AVBIAS	RMSE	AVBIAS	RMSE	AVBIAS	RMSE	AVBIAS
25	b	$0.6425_{(4)}$	$0.1618_{(2)}$	$0.4474_{(1)}$	$0.3271_{(4)}$	$0.5026_{(3)}$	$0.1457_{(1)}$	$0.4519_{(2)}$	$0.3177_{(3)}$	$0.6933_{(5)}$	$0.4163_{(5)}$
	α	$1.2720_{(5)}$	$0.5332_{(5)}$	$0.5862_{(2)}$	$0.3663_{(2)}$	$1.1433_{(4)}$	$0.4944_{(4)}$	$0.6518_{(3)}$	$0.3825_{(3)}$	$0.4123_{(1)}$	$0.3113_{(1)}$
	λ	$0.5588_{(3)}$	$0.0718_{(1)}$	$0.7824_{(5)}$	$0.4260_{(5)}$	$0.4203_{(1)}$	$0.1659_{(2)}$	$0.6622_{(4)}$	$0.4218_{(4)}$	$0.4721_{(2)}$	$0.3317_{(3)}$
	ω	$0.9851_{(4)}$	$0.1928_{(1)}$	$0.8178_{(3)}$	$0.5114_{(4)}$	$1.0330_{(5)}$	$0.2379_{(2)}$	$0.6784_{(1)}$	$0.3141_{(3)}$	$0.7146_{(2)}$	$0.5375_{(5)}$
	Sum of ranks		25		26		22		25		24
50	b	$0.2016_{(1)}$	$0.0281_{(2)}$	$0.4445_{(4)}$	$0.3243_{(4)}$	$0.2548_{(2)}$	$0.0250_{(1)}$	$0.4107_{(3)}$	$0.2975_{(3)}$	$0.5461_{(5)}$	$0.3940_{(5)}$
	α	$0.4390_{(3)}$	$0.1721_{(2)}$	$0.5146_{(5)}$	$0.3131_{(5)}$	$0.4573_{(4)}$	$0.1583_{(1)}$	$0.4219_{(2)}$	$0.2712_{(3)}$	$0.3508_{(1)}$	$0.2964_{(4)}$
	λ	$0.4269_{(3)}$	$0.1222_{(1)}$	$0.6045_{(5)}$	$0.3807_{(5)}$	$0.4186_{(2)}$	$0.1511_{(2)}$	$0.4916_{(4)}$	$0.3116_{(4)}$	$0.3415_{(1)}$	$0.2615_{(3)}$
	ω	$0.7567_{(3)}$	$0.1280_{(1)}$	$0.7851_{(4)}$	$0.4879_{(4)}$	$0.8459_{(5)}$	$0.1898_{(2)}$	$0.5142_{(1)}$	$0.2901_{(3)}$	$0.7412_{(2)}$	$0.5529_{(5)}$
	Sum of ranks		16		36		19		23		26
100	b	$0.15872_{(1)}$	$0.0126_{(1)}$	$0.4215_{(4)}$	$0.3025_{(4)}$	$0.2645_{(2)}$	$0.0278_{(2)}$	$0.3682_{(3)}$	$0.2149_{(3)}$	$0.5681_{(5)}$	$0.4106_{(5)}$
	α	$0.2822_{(1)}$	$0.0848_{(1)}$	$0.3219_{(3)}$	$0.2843_{(4)}$	$0.2868_{(2)}$	$0.0977_{(2)}$	$0.3514_{(4)}$	$0.2473_{(3)}$	$0.3922_{(5)}$	$0.3094_{(5)}$
	λ	$0.3232_{(1)}$	$0.0893_{(1)}$	$0.4128_{(4)}$	$0.2149_{(3)}$	$0.3907(3)$	$0.0877_{(2)}$	$0.5016_{(5)}$	$0.3193_{(5)}$	$0.3691_{(2)}$	$0.2796_{(4)}$
	ω	$0.5578_{(2)}$	$0.1164_{(1)}$	$0.6548_{(5)}$	$0.3273_{(4)}$	$0.5953_{(3)}$	$0.1309_{(2)}$	$0.3941_{(1)}$	$0.2048_{(3)}$	$0.6514_{(4)}$	$0.4318_{(5)}$
	Sum of ranks		9		31		18		27		35
200	b	$0.0394_{(1)}$	$0.0110_{(2)}$	$0.4036_{(5)}$	$0.3001_{(5)}$	$0.0399_{(2)}$	$0.0108_{(1)}$	$0.3645_{(3)}$	$0.2102_{(4)}$	$0.3789_{(4)}$	$0.1843_{(3)}$
	α	$0.1574_{(1)}$	$0.0221_{(1)}$	$0.2005_{(5)}$	$0.1977_{(4)}$	$0.1591_{(2)}$	$0.0281_{(2)}$	$0.2231_{4)}$	$0.1971_{(3)}$	$0.2541_{(5)}$	$0.2216_{(5)}$
	λ	$0.2214_{(2)}$	$0.0755_{(2)}$	$0.4230_{(5)}$	$0.2197_{(4)}$	$0.2889_{(3)}$	$0.0626_{(1)}$	$0.3578_{(4)}$	$0.2296_{(5)}$	$0.2158_{(1)}$	$0.1518_{(3)}$
	ω	$0.4060_{(1)}$	$0.0912_{(1)}$	$0.5497_{(5)}$	$0.2851_{(4)}$	$0.4284_{(3)}$	$0.1171_{(2)}$	$0.4125_{(2)}$	$0.2113_{(3)}$	$0.4751_{(4)}$	$0.3612_{(5)}$
	Sum of ranks		13		37		16		28		30
400	b	$0.0317_{(1)}$	$0.0080_{(1)}$	$0.2813_{(4)}$	$0.1567_{(4)}$	$0.0324_{(2)}$	$0.0093_{(2)}$	$0.3632_{(5)}$	$0.2011_{(5)}$	$0.2738_{(3)}$	$0.1199_{(3)}$
	α	$0.1132_{(1)}$	$0.0258_{(2)}$	$0.1532_{(3)}$	$0.1208_{(3)}$	$0.1550_{(4)}$	$0.0265_{(1)}$	$0.1145_{(2)}$	$0.1274_{(4)}$	$0.2613_{(5)}$	$0.2281_{(5)}$
	λ	$0.1438_{(2)}$	$0.0275_{(2)}$	$0.2123_{(4)}$	$0.1079_{(4)}$	$0.2001_{(3)}$	$0.0352_{3)}$	$0.0931_{(1)}$	$0.0091_{(1)}$	$0.2314_{(5)}$	$0.1722_{(5)}$
	ω	$0.3165_{(2)}$	$0.0134_{(1)}$	$0.3794_{(4)}$	$0.1822_{(4)}$	$0.3284_{(3)}$	$0.0960_{(3)}$	$0.2245_{(1)}$	$0.0907_{(2)}$	$0.4621_{(5)}$	$0.3512_{(5)}$
	Sum of ranks		12		30		21		21		36
800	b	$0.0230_{(2)}$	$0.0050_{(1)}$	$0.1302_{(4)}$	$0.0963_{(4)}$	$0.0222_{(1)}$	$0.0067_{(2)}$	$0.3120_{(5)}$	$0.1514_{(5)}$	$0.1115_{(3)}$	$0.0817_{(3)}$
	α	$0.0903_{(3)}$	$0.0220_{(4)}$	$0.1302_{(5)}$	$0.1045_{(5)}$	$0.0664_{(2)}$	$0.0069_{(1)}$	$0.0516_{(1)}$	$0.0145_{(3)}$	$0.1115_{(4)}$	$0.0112_{(2)}$
	λ	$0.0914_{(3)}$	$0.0009_{(1)}$	$0.1302_{(5)}$	$0.0324_{(4)}$	$0.1161_{(3)}$	$0.0147_{(3)}$	$0.0454_{(2)}$	$0.0021_{(2)}$	$0.0150_{(1)}$	$0.0068_{(5)}$
	ω	$0.2567_{(5)}$	$0.0298_{(3)}$	$0.2154_{(2)}$	$0.1162_{(4)}$	$0.2362_{(3)}$	$0.0182_{(2)}$	$0.1452_{1)}$	$0.0102_{(1)}$	$0.2416_{(4)}$	$0.1723_{(5)}$
	Sum of ranks		22		33		18		20		27

Table 6. Rankings of Estimation Methods for TL-HT-W Distribution across Different Values for the Model Parameters

Parameters	n	MLE	CVM	OLS	WLS	AD
$b = 0.8, \alpha = 0.8, \lambda = 1.5, \omega = 2.2$	25	4	5	1	3	2
	50	1	5	2	4	3
	100	1	5	3	4	2
	200	1	5	2	3	4
	400	1	2	3	4	5
	800	1	3	2	4	5
$b = 0.2, \alpha = 0.3, \lambda = 0.2, \omega = 2.4$	25	3.5	5	1	3.5	2
	50	1	5	2	3	4
	100	1	4	2	3	5
	200	1	5	2	3	4
	400	1	4	2.5	2.5	5
	800	3	5	1	2	4
	Sum of ranks	19.5	53	23.5	39	45
	Total rank	1	5	2	3	4

8. Applications

Real data examples were used to fit the TL-HT-W distribution, which belongs to the TL-HT-G family via R (version 4.4.1) package. The TL-HT-W model was contrasted with six non-nested models, which encompassed prominent heavy-tailed distributions. These competing distributions are: Kumaraswamy-Weibull (KW) by Cordeiro et al. [23], type I heavy-tailed Weibull (TIHTW) by Zhao et al. [20], heavy-tailed beta power transformed

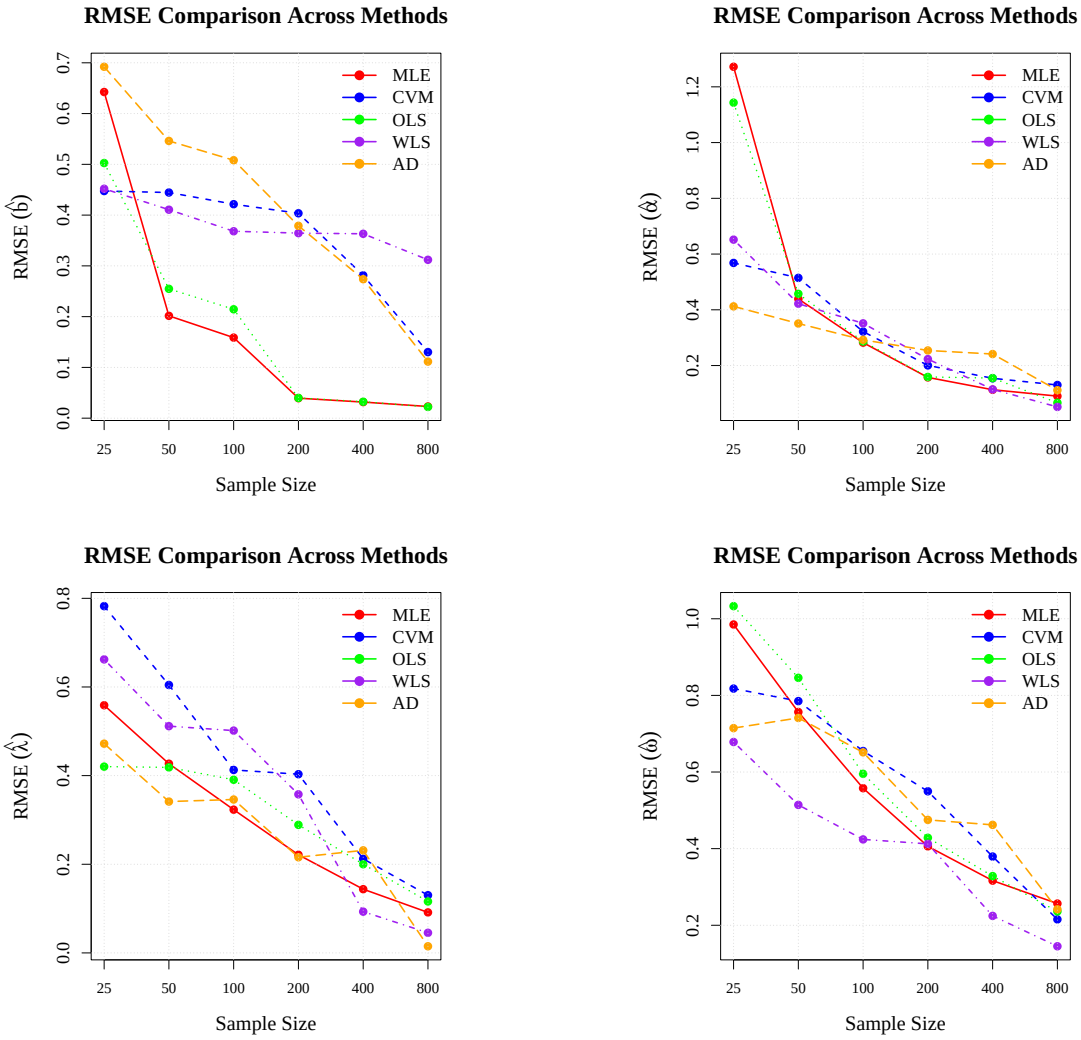

Figure 8. Plots of RMSEs for estimation of TL-HT-W distribution parameters for $b = 0.2, \alpha = 0.3, \lambda = 0.2, \omega = 2.4$ respectively.

Weibull pioneered by Zhao et al. [24], Weibull-Lomax (WL) by Tahir et al. [25], odd exponentiated half logistic Burr XII (HLBXII) by Aldahlan and Afify [26], and the exponential Lindley odd log-logistic Weibull (ELOLLW) by Korkmaz et al. [27] distributions. Please refer to the **web appendix** for the probability density functions of the distributions used in the comparisons.

Several goodness-of-fit (GoF) statistics were utilized for the comparison of different models, including: -2 log-likelihood ($-2\log(L)$), Akaike Information Criterion ($AIC = 2p - 2\log(L)$), Consistent Akaike Information Criterion ($CAIC = AIC + 2\frac{p(p+1)}{n-p-1}$), and Bayesian Information Criterion ($BIC = p\log n - 2\log(L)$), where n represents the number of observed parameters, while the number of calculated parameters is p. These statistics were utilized to identify the best-fitting model for a given dataset. The preferred model was identified based on having the highest p-value for the Kolmogorov-Smirnov (K-S) statistic and the lowest value for the selected GoF statistical criteria. Probability plots were also used to evaluate the GoF between the theoretical probability

distribution and an observed data set. The sum of squares (SS) obtained from the probability plots were used to assess the proximity between the fitted distribution and the observed data. SS is given by

$$SS = \sum_{r=1}^{n} \left[F_{TL-HT-W}(y_{(r)}; \hat{b}, \hat{\alpha}, \hat{\lambda}, \hat{\omega}) - \left(\frac{r - 0.375}{n + 0.25} \right) \right]^2, r = 1, 2, ..., n,$$

where $y'_{(r)}s$ represents the ordered values of the observed data.

The R software's nonlinear minimization (**nlm**) function was used to estimate the TL-HT-W model parameters. Parameter estimates were accompanied by their corresponding standard errors (SEs), which were displayed in parentheses. Profile log-likelihood plots were presented on all data sets to display the relationship between a parameter of interest and the TL-HT-W likelihood function and to demonstrate that the individual parameters are global maximums. Furthermore, the analysis encompassed the illustration of probability plots, fitted densities, empirical cumulative distribution function (ECDF), Kaplan-Meier (K-M) survival curves, scaled plots of total time on test (TTT), and plots illustrating the hrf.

8.1. Leukaemia Data

This data shows the remission times (measured in weeks) for a cohort of 30 patients diagnosed with leukaemia, a form of blood cancer. These patients underwent similar therapeutic interventions as part of their treatment. This information is available in Lawless by Lee [28] and the data is given in the **web appendix**. Both complete and censored observations are analyzed.

8.1.1. Leukaemia Data: Complete Case This subsection contains the parameter estimates, SEs of the estimates (in parentheses), GoF statistics, fitted densities, probability plots, K-M survival plot, ECDF plot, TTT scaled and hrf plots for the complete leukaemia data.

Table 7. **Parameter Estimates and GoF Statistics for Leukemia Data**

					Statistics					
Distribution	Estimates and SEs				-2log(L)	AIC	CAIC	BIC	K−S	p−value
TL-HT-W	b 4.4115 (3.01×10^{-3})	α 24.6120 (2.12×10^{-5})	λ 4.82×10^{-4} (6.65×10^{-5})	ω 0.49995 (0.0715)	195.9402	203.9402	205.9402	208.8157	0.0915	0.985
HLBXII	α 0.3936 (0.1294)	λ 0.0120 (0.0183)	a 1.1625 (0.3588)	b 1.1099 (0.4131)	210.3938	218.3938	220.3938	223.2693	0.1558	0.5785
ELOLLW	β 0.0011 (0.3925)	λ 0.0681 (0.0384)	θ 0.7916 (0.0034)	γ 0.9592 (0.1442)	197.4580	205.4580	207.4580	210.3335	0.1094	0.9258
WL	a 11.1060 (1.61×10^{-6})	b 10.7060 (2.78×10^{-5})	α 0.0463 (6.42×10^{-3})	β 6.02×10^{-5} (1.10×10^{-4})	197.9067	205.9067	207.9067	210.7821	0.1441	0.6769
TIHTW	α 0.9726 (3.94×10^{-10})	λ 49.7130 (4.75×10^{-12})	ω 2.39×10^{-5} (4.88×10^{-6})	-	199.9802	203.9802	205.9231	209.6368	0.1065	0.9394
HTBPTW	α 0.3499 (0.0607)	γ 0.9917 (0.2797)	β 3.03×10^{-4} (9.86×10^{-4})	-	199.1639	204.9639	206.1068	208.8205	0.1266	0.8181
KW	a 32.0271 (1.9288)	b 1.11×10^{4} (3.52×10^{-4})	α 7.7128 (0.6667)	β 0.0647 (7.79×10^{-3})	196.7970	204.7970	206.7970	209.6725	0.1004	0.9627
TLWLx	a 0.0816 (0.0130)	b 1.11×10^{3} (0.0651)	α 2.1474 (0.7894)	θ 10.5980 (11.0200)	197.0183	205.0182	207.0182	209.8937	0.1063	0.9401

Table [7] gives the MLEs with their corresponding SEs (in parentheses) of the unknown parameters for the TL-HT-W distribution obtained by maximizing the loglikelihood function in Equation (14) on leukaemia data. Figure [9] (a-d) clearly shows that the TL-HT-W parameters on leukaemia data are global maximums. The 95% asymptotic confidence intervals for the model parameters are $b \in [4.4115 \pm 6.23\times10^{-3}]$, $\alpha \in [24.6120 \pm 5.74$

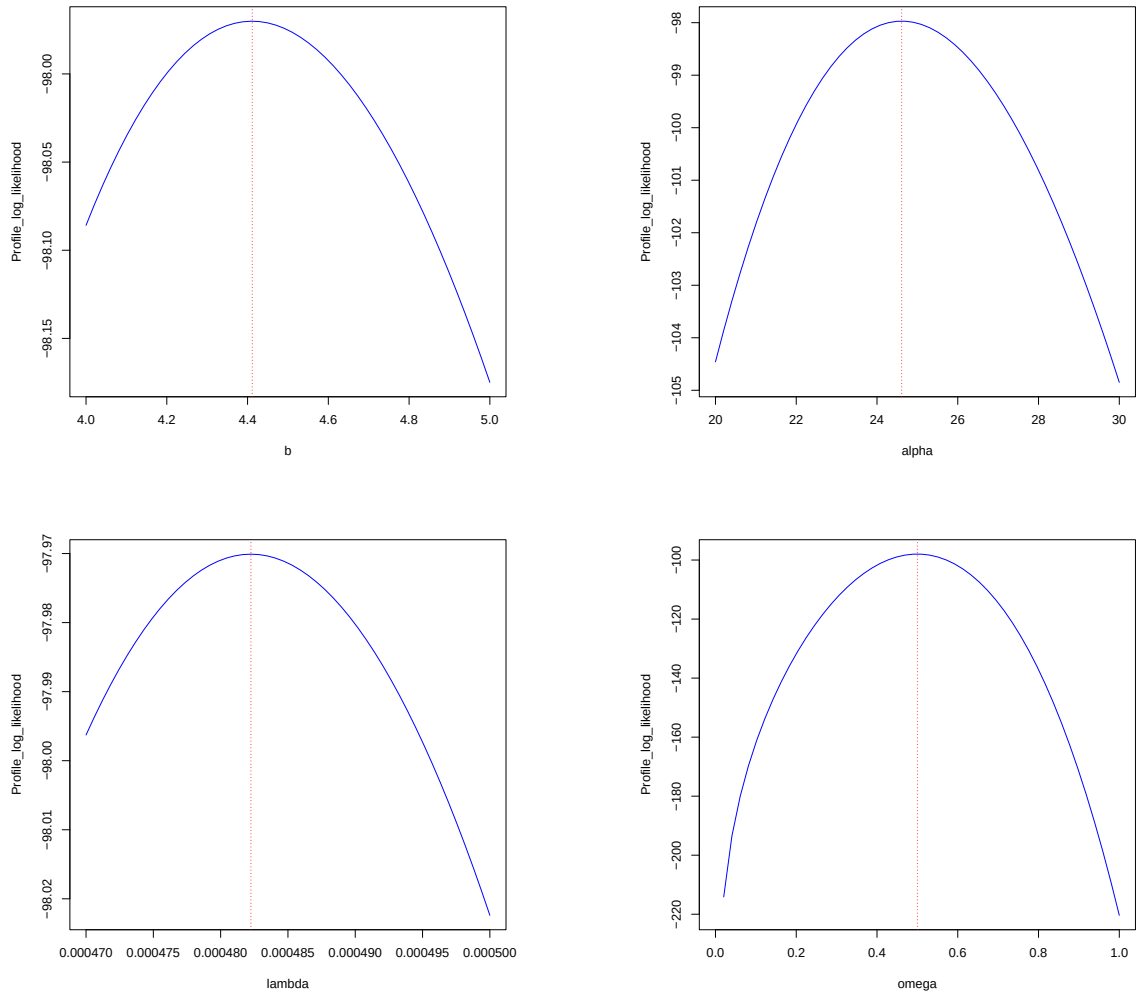

Figure 9. Profile log-likelihood plots of the TL-HT-W: Leukaemia data

$\times 10^{-5}]$, $\lambda \in [4.82\times10^{-4}\pm2.13\times10^{-4}]$ and $\omega \in [0.49995 \pm 0.1421]$, respectively.

The TL-HT-W model is superior to the several non-nested models that were taken into consideration, according to the GoF statistics and K-S p-values obtained on leukaemia data. In Figure [10] (a), the estimated density functions are presented, while panel (b) displays the corresponding probability plots. The integrated evaluation of both graphical analyses demonstrates that the TL-HT-W distribution provides a statistically superior GoF compared to the non-nested competing models for the leukaemia dataset.
Figures [11] (a) and (b) illustrates the comparison of the fitted and observed ECDF and K-M survival curves for leukaemia data. The TL-HT-W distribution exhibits close correspondence with the observed data, as evidenced by its close fit to the ECDF and K-M survival curves. The close fit of the TL-HT-W distribution to the observed ECDF and K-M survival curves for leukaemia indicates its validity as a model for survival data, enhancing its predictive power for patient prognosis. These findings may also encourage further research into its applications in other medical conditions and facilitate comparisons with other survival models.

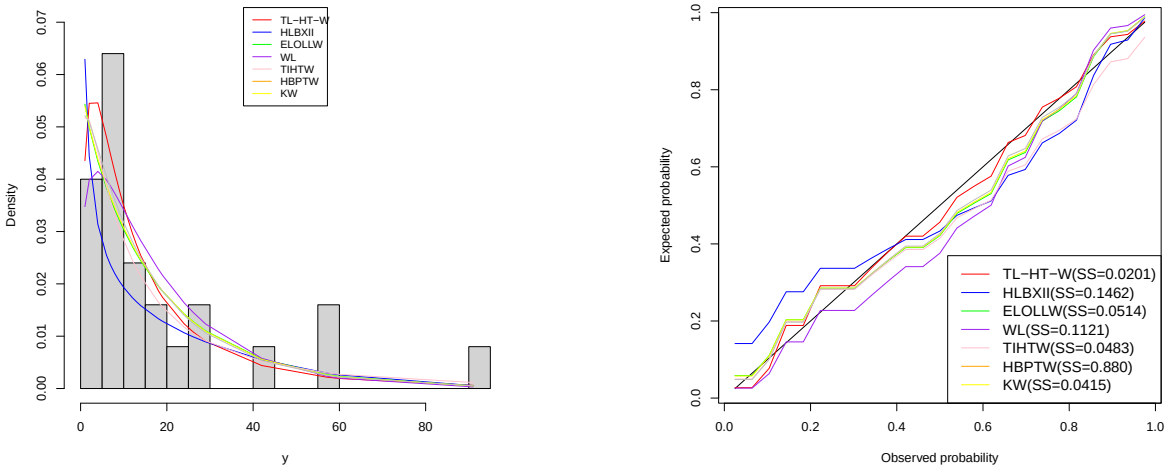

(a) **(b)**

Figure 10. Density (a) and probability plots (b) of fitted distributions for leukaemia data

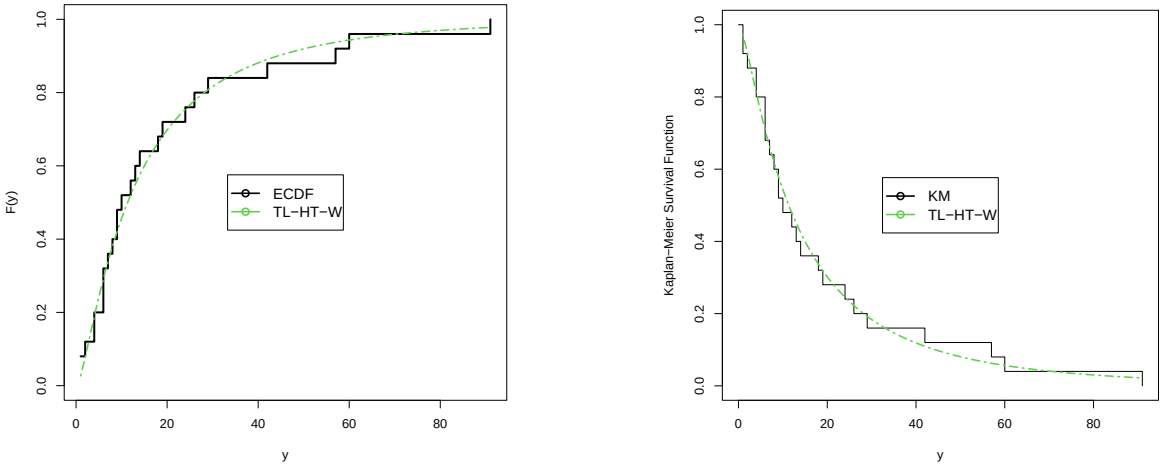

(a) **(b)**

Figure 11. Fitted ECDF curve (a) and K-M plots (b) for leukaemia data

The scaled TTT and hrf plots in Figure [12] (a) and (b) depict an inverted bathtub hazard rate shape for leukaemia data. The inverted bathtub hazard rate for leukaemia indicates an initial high risk of failure that decreases over time but may rise again, highlighting the need for effective early interventions and ongoing monitoring. An accurate model can identify critical intervention points, allowing clinicians to tailor treatments and optimize patient outcomes through proactive strategies and personalized care.

8.1.2. Leukaemia Data: Censored Case This section contains parameter estimates and GoF statistics for leukaemia censored data. The data is in the **appendix**.
Table [8] gives the MLEs with their corresponding SEs (in parentheses) of the unknown parameters for the TL-HT-W distribution obtained by maximizing the loglikelihood function in Equation (15). The table provides

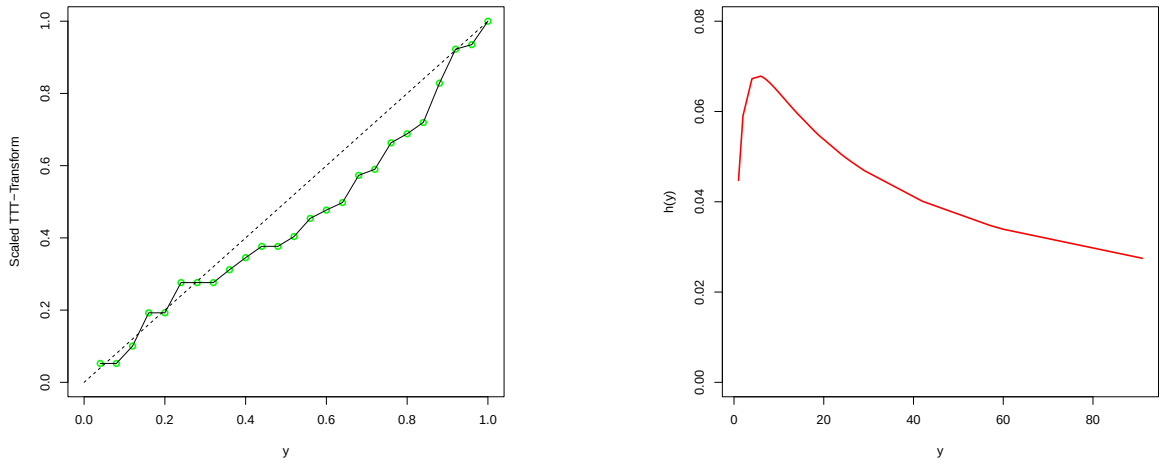

(a) **(b)**

Figure 12. Scaled TTT (a) and hrf plots (b) for leukaemia data

Table 8: **Parameter Estimates and GoF Statistics for Leukaemia Data (Censored Case)**

Distribution	Estimates and SEs				Statistics			
					-2log(L)	AIC	CAIC	BIC
	b	α	λ	ω				
TL-HT-W	100.1300	20.4661	4.02×10^{-3}	0.1631	210.0869	218.0869	219.6869	223.6917
	(8.11×10^{-6})	(9.62×10^{-6})	(2.76×10^{-4})	(0.0244)				
	α	λ	a	b				
HLBXII	0.2877	5.94×10^{-4}	3.2294	0.5431	218.6445	226.6445	228.2445	232.2493
	(0.0659)	(5.91×10^{-4})	(0.7848)	(0.1341)				
	β	λ	θ	γ				
ELOLLW	478.8100	264.8800	0.0159	0.5478	211.4107	219.4107	221.0107	225.0155
	(3.66×10^{-9})	(3.57×10^{-7})	(0.0125)	(0.0870)				
	a	b	α	β				
WL	11.1070	9.9917	0.0534	6.09×10^{-4}	219.4256	227.4256	229.0256	233.0304
	(4.09×10^{-6})	(1.34×10^{-4})	(0.0103)	(1.31×10^{-3})				
	α	λ	ω					
TIHTW	0.1655	11.9700	3.60×10^{-3}	-	262.7419	268.7419	269.6650	272.9455
	(0.0332)	(3.28×10^{-6})	(8.32×10^{-4})					
	α	γ	β					
HTBPTW	0.8296	0.0586	1.001	-	212.4520	218.8520	219.7551	222.6556
	(0.1369)	(0.0310)	(1.1768)					
	a	b	α	β				
KW	10.5119	245.4968	0.0141	0.1245	211.6359	219.6359	221.2359	225.2407
	(9.7561)	(0.0648)	(0.0828)	(0.0693)				
	a	b	α	θ				
TLWLx	4.0272	1.11×10^{3}	0.0294	398.3900	210.1903	218.1903	220.2655	227.3093
	(6.33×10^{-6})	(2.43×10^{-9})	(8.66×10^{-4})	(9.46×10^{-9})				

important information about the parameter estimates and their associated uncertainties, derived from the analysis of censored data. The 95% asymptotic confidence intervals for the model parameters are $b \in [100.1300 \pm 1.59\times10^{-5}]$, $\alpha \in [20.4660 \pm 1.88\times10^{-5}]$, $\lambda \in [4.02\times10^{-3} \pm 5.42\times10^{-4}]$ and $\omega \in [0.1631 \pm 0.0478]$, respectively. The TL-HT-W mode1 out-performs the non-nested models that were considered according to the GoF obtained on leukaemia censored data.

8.2. Bladder Cancer Data

The dataset comprises remission times (measured in months) for a random selected sample of 137 patients diagnosed with bladder cancer. This dataset was recently analyzed by Klakattawi [29] and can be found in the **web appendix** of the study. Complete and censored observations are both analyzed.

8.2.1. Bladder Cancer Data: Complete Case This subsection contains the parameter estimates, SEs of the estimates (in parentheses) GoF statistics, fitted densities, probability plots, K-M survival plot, ECDF plot, scaled TTT plot and hazard rate plot for the complete bladder cancer data.

The MLEs along with their SEs are shown in Table [9]. Figure [13] (a-d) demonstrates clearly that the TL-HT-W parameters on bladder cancer data are global maximums. The 95% asymptotic confidence intervals for the model parameters are $b \in [1.3213 \pm 1.9641]$, $\alpha \in [0.1491 \pm 0.3280]$, $\lambda \in [1.4606 \pm 1.0942]$ and $\omega \in [0.6535 \pm 0.4017]$, respectively.

Table 9. **Parameter Estimates and GoF Statistics for Bladder Cancer Data**

									Statistics	
Distribution	Estimates and SEs				-2log(L)	AIC	CAIC	BIC	K−S	p−value
	b	α	λ	ω						
TL-HT-W	1.3213	0.1491	1.4606	0.6535	819.1353	827.1353	827.4605	838.5434	0.0336	0.9987
	(1.0021)	(0.1674)	(0.5583)	(0.2049)						
	α	λ	a	b						
HLBXII	0.3925	0.0274	3.6829	0.3660	881.8121	889.8121	890.1373	901.2202	0.1166	0.0616
	(0.0649)	(0.0187)	(1.0211)	(0.0976)						
	β	λ	θ	γ						
ELOLLW	0.0011	0.1434	0.7185	1.0478	828.1738	836.1738	836.4990	847.5819	0.0700	0.5570
	(0.0988)	(7.6581)	(40.2103)	(0.0676)						
	a	b	α	β						
WL	111.2400	6.2349	0.0532	6.47×10^{-3}	823.4118	831.4118	831.7370	842.8199	0.0569	0.8012
	(4.63×10^{-3})	(2.4122)	(9.61×10^{-3})	(0.0194)						
	α	λ	ω							
TIHTW	1.0872	32.3970	8.35×10^{-5}	-	826.7345	832.7345	832.9280	841.2905	0.0692	0.5729
	(1.67×10^{-9})	(3.99×10^{-11})	(7.63×10^{-6})							
	α	γ	β							
HTBPTW	1.0478	0.0939	1.001	-	828.1238	834.1738	834.3673	842.7298	0.0700	0.5570
	(0.0676)	(0.0191)	(0.7282)							
	a	b	α	β						
KW	42.8910	1.11×10^{4}	280.0470	0.0624	824.2797	832.2797	832.6049	843.6878	0.0595	0.7551
	(1.8680)	(2.73×10^{-4})	(0.0234)	(2.84×10^{-3})						
	a	b	α	θ						
TLWLx	0.0719	1.11×10^{3}	5.5368	1.6091	822.2185	830.2185	830.5437	841.6266	0.0486	0.9230
	(1.91×10^{-3})	(3.94×10^{-4})	(1.1265)	(0.6068)						

Based on GoF statistics and K-S p-values calculated for bladder cancer data, the TL-HT-W model demonstrates superior performance compared to the considered non-nested models. This conclusion is further supported by Figure 14 (a) and (b), where the TL-HT-W distribution shows a better fit than alternative models.
Figure 15 demonstrates the TL-HT-W distribution's exceptional fit to bladder cancer survival data, with panel (a) aligning with the ECDF and panel (b) mirroring the K-M survival curve. This dual concordance underscores the model's reliability for survival analysis, offering a foundation for refining prognostic tools and optimizing individualized treatment protocols.
Panels (a) and (b) in Figure 16 reveal an inverted bathtub-shape hrf for bladder cancer survival data. Accurate modeling of this characteristic hazard profile is critical for improving risk stratification and guiding personalized treatment strategies in clinical oncology. The TL-HT-W distribution, which effectively captures this behavior, emerges as a promising candidate for enhancing prognostic accuracy and therapeutic decision-making in bladder cancer management.

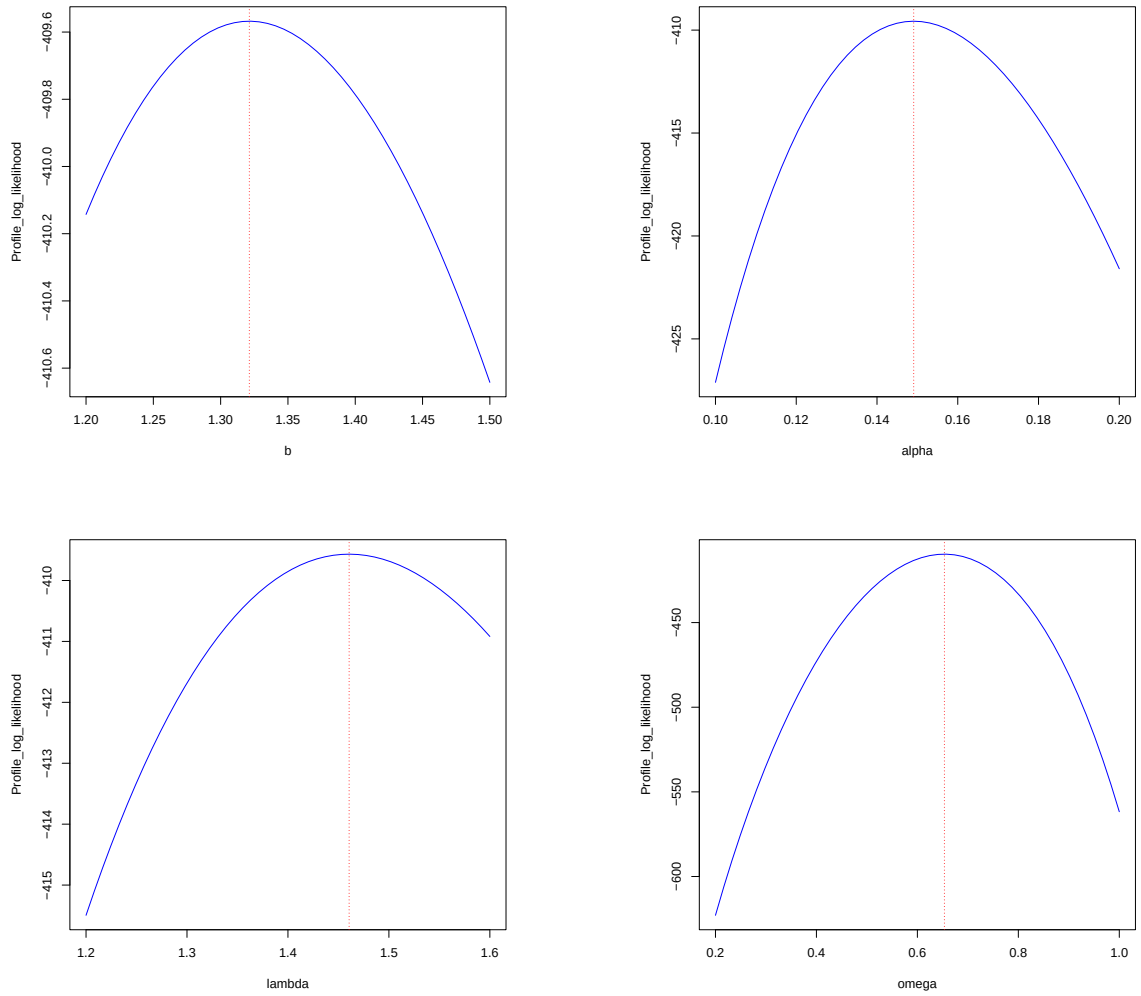

Figure 13. Profile log-likelihood plots of the TL-HT-W: Bladder cancer data

8.2.2. Bladder Cancer Data: Censored Case This section contains parameter estimates and GoF statistics for the censored data. The data is in the **appendix**.
Table [10] gives the MLEs with their corresponding SEs (in parentheses) of the unknown parameters for the TL-HT-W distribution for the censored data found by optimising the log-likelihood function in Equation (15). The TL-HT-W mode1 out-performs the non-nested models that were considered according to the GoF obtained on bladder cancer censored data. Asymptotic confidence intervals at 95% level for the model parameters are $b \in [1.2220 \pm 1.8363]$, $\alpha \in [0.1284 \pm 0.2951]$, $\lambda \in [1.4846 \pm 1.0327]$ and $\omega \in [0.6683 \pm 0.4425]$, respectively.

9. Results and Discussion

This article introduced and examined a new statistical distribution known as the Topp-Leone heavy-tailed-G (TL-HT-G) FoDs. The article included the derivation of various statistical properties and investigated five distinct techniques for quantifying the parameters of the TL-HT-W distribution, which belongs to the TL-HT-G family.

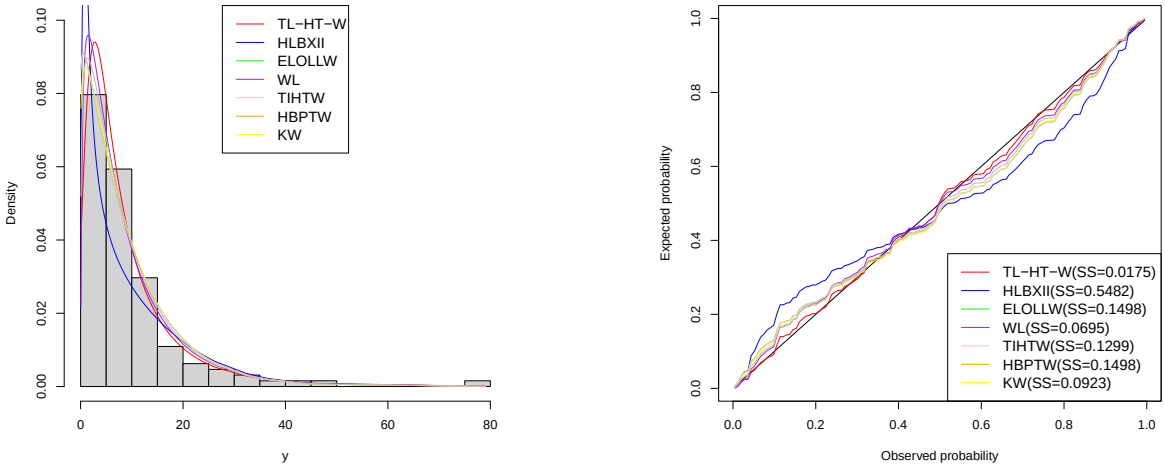

(a) **(b)**

Figure 14. Visualization of fitted distributions through density (a) and probability plots (b) for bladder cancer data Scaled TTT (a) and hrf plots (b) for leukaemia data

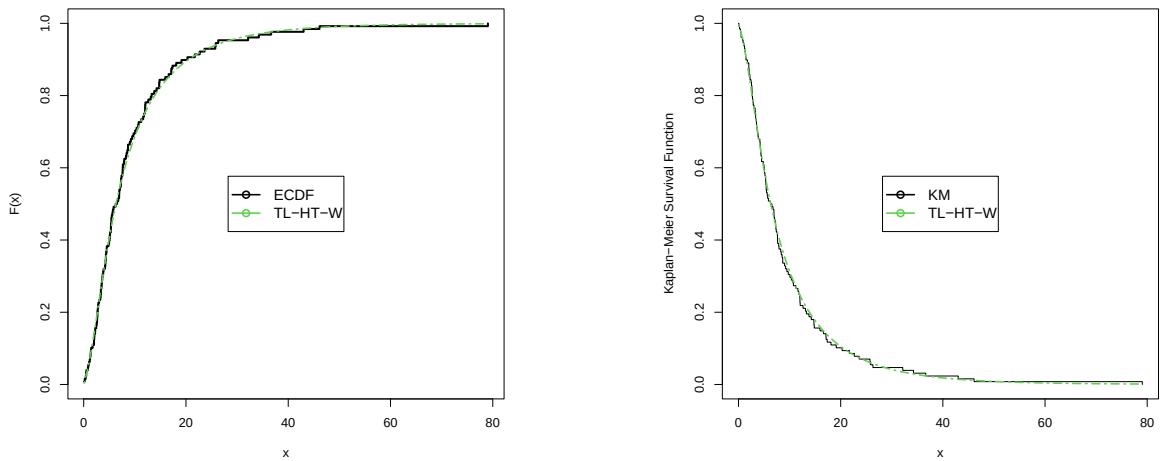

(a) **(b)**

Figure 15. Fitted ECDF curve (a) and K-M plots (b) for bladder cancer data

Results from Monte Carlo simulations showed that the TL-HT-W distribution demonstrated stability with modest AVBIAS and RMSE values, along with improved estimation accuracy with larger sample sizes across all methods. Furthermore, MLE provided the most accurate parameter estimates, leading to the decision to use MLE for estimating the distribution's unknown parameters.

We also derived actuarial risk measures and conducted numerical simulations for these measures. After standardizing all distributions to a common median to remove confounding scale effects, the numerical simulations demonstrated that the TL-HT-W distribution exhibits genuinely heavier tails compared to the

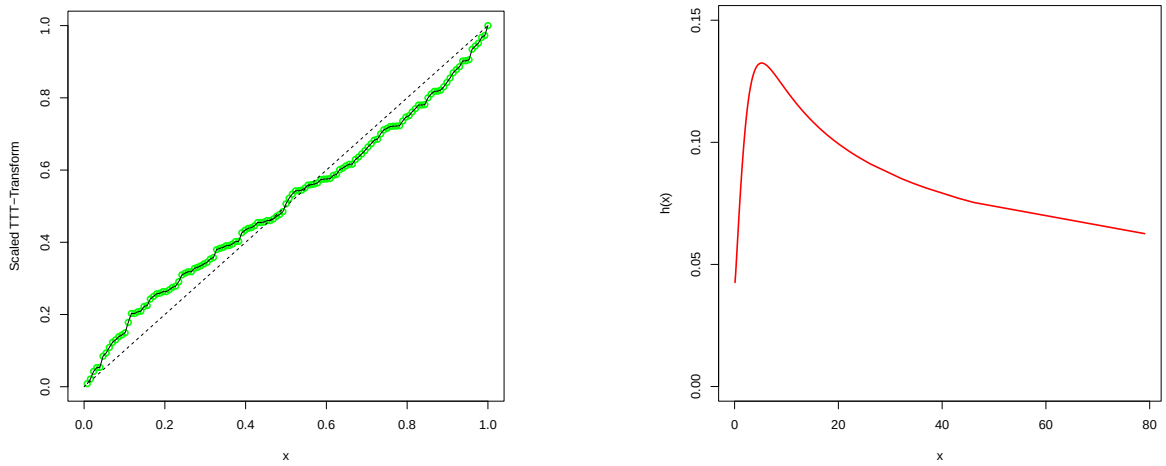

(a) **(b)**

Figure 16. Fitted TTT (a) scaled and hrf plots (b) for bladder cancer data

Table 10. **Parameter Estimates and GoF Statistics for Bladder Cancer Data (Censored Case)**

					Statistics			
Distribution	Estimates and SEs				-2log(L)	AIC	CAIC	BIC
	b	α	λ	ω				
TL-HT-W	1.2220	0.1284	1.4846	0.6683	836.2526	844.2526	836.3278	844.8121
	(0.9369)	(0.1506)	(0.5269)	(0.2258)				
	α	λ	a	b				
HLBXII	0.3942	0.0222	3.6690	0.3782	897.0698	905.0698	905.3728	916.7497
	(0.0662)	(0.0162)	(1.0234)	(0.1007)				
	β	λ	θ	γ				
ELOLLW	455.8200	1.6800	0.2836	0.7236	839.7372	847.7372	848.0402	859.4171
	(6.81×10^{-4})	(6.4202)	(0.7839)	(0.0467)				
	a	b	α	β				
WL	93.8530	6.2738	0.0538	0.0063	840.3958	848.3958	848.7837	860.1606
	(1.78×10^{-7})	(3.79×10^{-5})	(3.41×10^{-3})	(3.02×10^{-3})				
	α	λ	ω					
TIHTW	1.1983	3.3565	0.0064	-	840.7505	846.7505	846.9310	848.4453
	(0.0809)	(1.9031)	(0.0074)					
	α	γ	β					
HTBPTW	1.0536	0.0866	1.001	-	844.8293	850.8293	851.0098	852.5241
	(0.0681)	(0.0177)	(0.6889)					
	a	b	α	β				
KW	3.8933	2.6806	0.1999	0.4749	838.2904	846.2904	846.5934	857.9703
	(5.5562)	(7.8578)	(0.2305)	(0.5466)				
	a	b	α	θ				
TLWLx	0.0714	109.7600	5.5868	1.5783	839.2987	846.2987	846.3737	857.8582
	(1.89×10^{-3})	(4.15×10^{-4})	(1.1802)	(0.6051)				

Kumaraswamy-Weibull and standard Weibull distributions, as evidenced by larger standardized VaR, TVaR, and TV values at extreme quantiles. The type-I heavy-tailed Weibull showed comparable tail ratios, but the TL-HT-W maintained more consistent heavy-tail behavior across quantile levels. Critically, the tail heaviness of the TL-HT-W distribution is explicitly tunable via the parameter α (Corollary 1), providing practitioners with direct control over tail behavior. These findings confirm the TL-HT-W's suitability for heavy-tailed data modeling in actuarial science, particularly for high-quantile risk assessment where accurate tail estimation is paramount.

The TL-HT-W distribution provides reliable parameter estimates for both complete and censored leukemia

and bladder cancer data, as evidenced by favorable GoF statistics and high K-S p-values, underscoring its robustness in modeling remission times and enhancing clinical applicability. Its strengths include significant modeling flexibility and strong predictive power for effective forecasting and decision-making. However, while versatile, it may not accurately represent all real-world data, increasing the risk of misinterpretation if incorrectly applied.

We recommend extending the new FoDs through bivariate extensions and utilizing copulas for future research. Additionally, integrating regression and cure rate frameworks for covariate-adjusted survival analysis would further enhance the utility of the TL-HT-G family across high-stakes applications in actuarial science, clinical survival analysis, and reliability engineering.

To view the appendix, please click on the link.
https://drive.google.com/file/d/1vLDBrls8TR_sVqdxMBfSAB1pi3hFCruz/view?usp=sharing

Declaration of conflict of interest

The authors report there are no competing interests to declare.

Data availability

The data that support the findings of this study are provided in the web appendix.

Declaration of funding

This research did not receive any specific grant from funding agencies in the public, commercial, or not-for-profit sectors. The authors have no sponsorship or funding to declare, and no sponsor has had any role in the preparation, writing, or decision to submit this article.

Funding Statement

Thi s research did not receive any sponsorship from individuals or organizations.

Declaration of competing interest

The authors assert that there are no conflicts of interest among them.

REFERENCES

1. Ickowicz, A., and Sparks, R., *Modelling hospital length of stay using convolutive mixtures distributions*, Statistics in medicine, vol. 36, no. 1, pp. 122–135, 2017.
2. Subbiah, H., Subbiah, M., and Srinivasan, M. R., *Fitting length of stay in hospitals using transformed distributions*, Communications in Statistics: Case Studies, Data Analysis, vol. 4, no. 1, pp. 1–8, 2018.
3. Bhati, D., and Ravi, S., *On generalized log-moyal distribution: A new heavy tailed size distribution*, Insurance: Mathematics and Economics, vol. 79, no. 1, pp. 247–259, 2018.
4. Al-Shomrani, A., Arif, O., Shawky, A., Hanif, S., and Shahbaz, M. Q., *Topp-Leone family of distributions: Some properties and application*, Pakistan Journal of Statistics and Operation Research, pp. 443–451, 2016.

5. Oluyede, B., Dingalo, N., and Chipepa, F., *The Topp-Leone-Harris-G family of distributions with applications*, International Journal of Mathematics in Operational, vol. 24, no. 4, pp. 554–582, 2023.
6. Chinofunga, P. T., Oluyede, B., and Chipepa, F., *The New Topp-Leone-Marshall-Olkin-Gompertz-G family of distributions: Properties, different estimation techniques and applications on censored and complete data*, Statistics, Optimization & Information Computing , vol. 14, no. 1, pp. 77–104, 2025.
7. Nicodéme Atchadé, M., AG Nb́ouké, M., Djibril, A. M., Al Mutairi, A., Mustafa, M. S., Hussam, E., Alsuhabi, H., and Nassr, S. G., *A new Topp-Leone Kumaraswamy Marshall-Olkin generated family of distributions with applications*, Heliyon, vol. 10, no. 2, 2024.
8. Eghwerido, J. T., and Ikechukwu Agu, F., *The statistical properties and applications of the alpha power Topp-Leone-G distribution*, Heliyon, vol. 8, no. 6, 2022.
9. Nkomo, W., Oluyede, B., and Chipepa, F., *Topp-Leone type I heavy-tailed-G power series class of distributions: Properties, risk measures, and applications*, Statistics, Optimization & Information Computing, vol. 13, no. 1, pp. 88–110, 2025.
10. Ahmed, M. T., Khaleel, M. A, and Khalaf, E. K., *The new distribution (Topp Leone Marshall Olkin-Weibull) properties with an application*, Periodicals of Engineering and Natural Sciences (PEN), vol. 8, no. 2, pp. 684–692, 2020.
11. Chipepa, F., and Oluyede, B., *The Topp-Leone odd exponential half logistic-G family of distributions: Model, properties and applications*, Pakistan Journal Statistics, vol. 37, no. 3, pp. 253–277, 2021.
12. Moakofi, T., Oluyede, B., and Chipepa, F., *Type II exponentiated half-logistic Topp-Leone Marshall-Olkin-G family of distributions with applications*, Heliyon, vol. 7, no. 12, 2021.
13. Moakofi, T., Oluyede, B., and Gabanakgosi, M., *The Topp-Leone odd Burr III-G family of distributions: Model, properties and applications*, Statistics, Optimization & Information Computing, vol. 10, no. 1, pp. 236–262, 2022.
14. Chipepa, F., Oluyede, B., and Makubate, B., et-al *The Topp-Leone-Marshall-Olkin-G family of distributions with applications*, International Journal of Statistics and Probability, vol. 9, no. 4, pp. 15–32, 2020.
15. Chesneau, C., Sharma, V. K., and Bakouch, H. S., *Extended Topp–Leone family of distributions as an alternative to beta and Kumaraswamy type distributions: Application to glycosaminoglycans concentration level in urine*, International Journal of Biomathematics, vol. 14, no. 2:2050088, 2021.
16. Mohammad, G, S., *A new weighted Topp-Leone family of distributions*, Statistics, Optimization & Information Computing, vol. 11, no. 3, pp. 615–628, 2023.
17. Oluyede, B., Chamunorwa, S., Chipepa, F., and Alizadeh, M., *The Topp-Leone Gompertz-G family of distributions with applications*, Journal of Statistics and Management Systems, vol. 25, no. 6, pp. 1399–1423, 2022.
18. Dingalo, N., Oluyede, B., and Chipepa, F., *The Topp-Leone-Gompertz-exponentiated half logistic-G family of distributions with applications*, Revista Colombiana de Estad´ıstica, vol. 46, no. 2:55, 2023.
19. Makubate, B., Rannona, K., Oluyede, B., and Chipepa, F., *The Topp Leone-G power series class of distributions with applications*, Pakistan Journal of Statistics and Operation Research, vol. 17, no. 4, pp. 827–846, 2021.
20. Zhao, W., Khosa, S. K., Ahmad, Z., Aslam, M., and Afify, A.Z., *Type-I heavy tailed family with applications in medicine, engineering and insurance*, PloS one, vol. 15, no. 8:e0237462, 2020.
21. Shaked, M., and Shanthikumar., J. G., *Stochastic orders*, Springer Science & Business Media, 2007.
22. Usman, A.U., Tukur, U., Suleiman, A., Abdulkadir, A., and Ibrahim., H., *The use of the weighted least squares method when the error variance is heteroscedastic*, Benin Journal of Statistics, vol. 2, pp. 85–93, 2019.
23. Cordeiro, G. M., Ortega, M. M., and Nadarajah, S., *The Kumaraswamy Weibull distribution with application to failure data*, Journal of the Franklin institute, vol. 347, no. 8, pp. 1399–1429, 2010.
24. Zhao, J., Ahmad, Z., Mahmoudi, Z., Hafez, E. H., and El-Din, M. M., *A new class of heavy-tailed distributions: Modeling and simulating actuarial measures*, Complexity, vol. 2021, no. 1:5580228, 2021.
25. Tahir, M. H., Cordeiro, G. M., Mansoor, M., and Zubair, M., *The Weibull-Lomax distribution: properties and applications*, Hacettepe Journal of Mathematics and Statistics, vol. 44, no. 2, pp. 455–474, 2015.
26. Aldahlan, M., and Afify, A. Z., *The odd exponentiated half-logistic Burr XII distribution*, Pakistan Journal of Statistics and Operation Research, 305–317, 2018.
27. Korkmaz, M. C., Yousof, H. M., and Hamedani, G. G., *The exponential Lindley odd log-logistic-G family: properties, characterizations and applications*, Journal of Statistical Theory and Applications, vol. 17, no. 3, pp. 554–571, 2018.
28. Lee, E. T., *Statistical methods for survival data analysis*, IEEE Transactions on Reliability, vol.35, 1st Edition, 1986.
29. Klakattawi, H. S., *Survival analysis of cancer patients using a new extended Weibull distribution*, Plos One, vol. 17, no. 2:e0264229, 2022.